Transportation Research Part C 158 (2024) 104447

Contents lists available at ScienceDirect

Transportation Research Part C

journal homepage: www.elsevier.com/locate/trc

Robust multi-equipment scheduling for U-shaped container terminals concerning double-cycling mode and uncertain operation time with cascade effects

Lei Cai [a,b,d], Wenfeng Li [a,b,*], Bo Zhou [c], Huanhuan Li [d], Zaili Yang [d,*]

[a] State Key Laboratory of Maritime Technology and Safety, Wuhan University of Technology, Wuhan 430063, PR China
[b] School of Transportation and Logistics Engineering, Wuhan University of Technology, Wuhan 430063, PR China
[c] School of Computer Science and Mathematics, Liverpool John Moores University, Liverpool John Moores Uniersity, L3 3AF, UK
[d] Liverpool Logistics, Offshore and Marine Research Institute, Liverpool John Moores University, Liverpool L3 3AF, UK

ARTICLE INFO

Keywords:
Port integrated multi-equipment scheduling
Dynamic scheduling
Uncertain operation time
U-shaped container terminal
Cascade effects

ABSTRACT

The integrated scheduling of quay cranes, internal vehicles, and yard cranes in container terminals aims to improve port operations and often requires scheduling robustness under uncertainty with cascade effects. In container terminal operations, uncertainty in equipment operating time poses challenges to effective scheduling, as even small fluctuations can create cascade effects throughout the operations, rendering the original schedule ineffective. This research aims to develop a new method that enables a balance between optimization and robustness in container terminal scheduling. Additionally, the double-cycling operation mode and U-shaped port layout, known for their improved efficiency in container terminals, are gaining increasing attention and hence are incorporated into this study. It creates a three-stage hybrid flow shop scheduling problem with bi-directional flows, waiting time, and uncertain operation time. To address the complex problem, a mixed integer programming model is proposed to characterize the integrated scheduling problem, and an index based on complex network structure entropy is designed to evaluate the anti-cascade effect as well as the robustness of the schedule. The index and *makespan* serve as the bi-objectives, transforming the original problem into a bi-objective optimization one. The non-dominated sorting genetic algorithm-II with appropriate coding and decoding rules is utilized to solve the model and obtain a set of Pareto frontier solutions. The feasibility of the new method is verified through a real case analysis. Specifically, comparative analysis with basic stochastic programming, basic robust optimization, triangular fuzzy programming, and maximum gap method are used to demonstrate the effectiveness of the new method. The paper also provides insightful practical implications for port managers, and the genericity of the method could also contribute to its practical values spreading to a wider scope of beneficiaries, such as manufacturing warehousing and distribution management.

* Corresponding authors at: State Key Laboratory of Maritime Technology and Safety, Wuhan University of Technology, Wuhan 430063, PR China (W. Li). Liverpool Logistics, Offshore and Marine Research Institute, Liverpool John Moores University, Liverpool L3 3AF, UK (Z. Yang)
E-mail addresses: liwf@whut.edu.cn (W. Li), Z.Yang@ljmu.ac.uk (Z. Yang).

https://doi.org/10.1016/j.trc.2023.104447
Received 10 September 2023; Received in revised form 27 November 2023; Accepted 28 November 2023

1. Introduction

Shipping transportation is responsible for 80 % of global trade cargos, making ports crucial logistics nodes in world trade (Li and Yang, 2023; Talley and Ng, 2022). Ports connect land and water transportation and have a significant impact on the economy of a region or a country (Li et al., 2023a). The use of containers has greatly reduced loading and unloading times, improving port efficiency (Guo et al., 2021). Equipment such as Quay Cranes (QCs), Yard Cranes (YCs), and Internal Vehicles (IV) supplement and facilitate container transport and operations in a container terminal (Yue et al., 2023; Zhen et al., 2018). However, the matter of using such equipment collectively and effectively influences efficient container handling and transportation, energy saving, greenhouse emissions reduction and decreased vessel turnover time (Li et al., 2022; Zhang et al., 2022b) and overall port competitiveness.

The general flow of containers through port handling equipment and space resources is illustrated in Fig. 1. In the past, research primarily focused on the scheduling of individual resources or equipment, such as berth allocation problem, yard allocation problem, QC Scheduling Problem (QCSP), IV Scheduling Problem (IVSP), and YC Scheduling Problem (YCSP). Nonetheless, due to the necessity for containers to undergo multiple fixed operations that can be processed by parallel equipment, resembling a hybrid flow-shop scheduling problem, there has been a growing interest in multi-stage resources or integrated equipment scheduling. This includes Berth Allocation and QC Assignment and Scheduling Problem (BACASP) (Na and Zhihong, 2009; He, 2016; He et al., 2021; Ji et al., 2022; Yu et al., 2023), integrated berth and yard space allocation (Zhen et al., 2022), QC and IV integrated scheduling problem (Hop et al., 2021; Zhen et al., 2019; Zhu et al., 2022), YC and IV integrated scheduling (Chen et al., 2020; Zhou et al., 2020; Hsu et al., 2021a, b), and QC, IV, and YC integrated scheduling problems (Zhuang et al., 2022) to further achieve global optimization.

In addition to integrated scheduling, adopting efficient operation modes such as a double-cycling mode can also optimize the allocation and scheduling of container terminal resources (Zhang et al., 2015; Tan et al., 2021). In the relevant literature, it is called bi-directional flows (Zhuang et al., 2022). As shown by the red arrows in Fig. 1, QCs, IVs, and YCs can form a simple double-cycling container flow. In this double-cycling mode, both container flow and transportation equipment meet the characteristics of the cycle, leading to the term “double-cycling” for this mode. The principal difference between the double-cycling operation mode and the traditional operation mode lies in the transportation sequence of the IV. In the double-cycling mode, an IV can transport an inbound container from the shoreside to the yard and then proceed to transport an outbound container from the yard to the shoreside. Conversely, in the traditional operation mode, the IV typically undertakes a single loaded journey between the yard and the shoreside. Double-cycling IVs transportation has been well applied in world-leading container ports (e.g. *Qingdao* in China). The double-cycling of IVs can reduce unnecessary no-load movement times effectively and save energy consumption. Although showing the attractiveness, the double-cycling has revealed a new research challenge on multi-equipment integrated scheduling in its practical applications.

Compared to traditional horizontal and vertical layouts of container terminals, a U-shaped container terminal model as an emerging port layout offers appealing advantages, evident by its pioneering implementation in *Qinzhou* Port and shows its huge potential to grow in container terminal developments. Fig. 2 illustrates a U-shaped terminal. The differences between the U-shaped layout and the traditional layout lie in that the U-shaped design improves its capacity to allow Intelligent Guided Vehicles (IGVs) better access the yard, enabling a larger number of unloading/loading points, while efficiently realizing the separation of the roads for IGVs and External Vehicles (EVs). This segregation reduces the number of crossroads, enabling a more efficient traffic flow within the terminal. As a result, the focus of this study is solely set to address the integrated scheduling problem of QCs, IGVs, and YCs, without the necessity to consider the impact of EVs or other external vehicles. Furthermore, even though the yard of a U-shaped terminal is perpendicular to the shoreline, it can function similarly to a yard that is parallel to the shoreline, allowing the IVs to travel deeper into the yard to easily arrive at specific bay positions. In contrast, in many terminals with perpendicular yards, IVs can only interact with

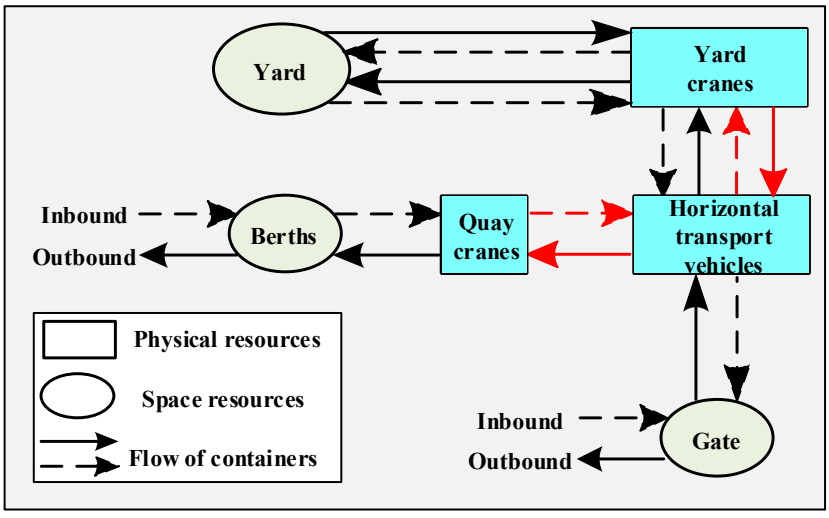

Fig. 1. The flow of containers in a container terminal.

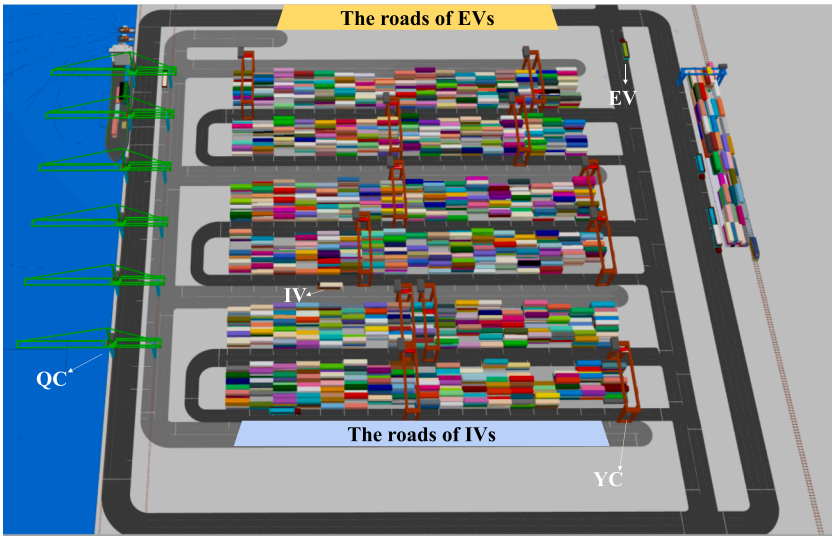

Fig. 2. Simplified 3D layout of a U-shaped container terminal.

YCs at the end of the yard, leading to unnecessary empty-load movements by the YCs. According to Niu et al. (2022), the energy consumption of YCs contributes to 25–30 % of the total energy costs of a container terminal, whereas the energy consumption of IVs accounts for only 1.04 % of the total energy consumption. Aligning the travel distance of IVs with that of YCs highlights the energy efficiency of IVs (He et al., 2015). Such advantages of the U-shaped terminals justify the significance of this study, revealing a significant emerging research question on how to coordinator multi-equipment for optimal operations in theory and the feasibility of the solution in a new terminal setting of high value in practice.

Due to the involvement of multiple scheduling equipment types at different stages of container operations, integrated scheduling exhibits a stronger coupling relationship between the operations within a schedule. However, this strong coupling could result in the scheduling being very fragile. As depicted in Fig. 3, various factors, such as weather conditions, collision avoidance, and equipment performance, can lead to deviations in the actual operation time, resulting in fluctuations and uncertainty (Xiang et al., 2017; He et al., 2019a; Tan and He, 2021). Although the deviation in a single operation may be minor, the accumulation of these small fluctuations can ultimately disrupt the entire scheduling plan due to the strong coupling relationship and the associated possible cascade effects. In the small-scale scheduling plan illustrated in Fig. 3, some operation time is shorter than expected, while others are longer, leading to an overall increase in the *makespan* by approximately 10 % compared to the expected duration. This phenomenon can be interpreted as a cascade effect caused by uncertain fluctuations in operating time. It is worth noting that in large-scale cases, these cascade effects become more pronounced, further highlighting the need for developing new robust scheduling strategies.

In conclusion, the integration of an increased number of unloading/loading points within the U-shaped layout, combined with the introduction of an additional mapping process to establish double-cycling pairs between inbound and outbound containers, significantly amplifies the intricacies and demands of this integrated scheduling problem. To address these complexities, it is essential to employ a more sophisticated matrix that represents the distances travelled by IVs between unloading/loading points. Furthermore, it is necessary to incorporate relevant variables and constraints that accurately depict the double-cycling operations. Regarding uncertainty, this port integrated scheduling problem addressed in this study can be conceptualized as a three-stage hybrid flow shop scheduling problem with bi-directional flows, waiting time, and uncertain operation time. Various approaches have been proposed by researchers to tackle the challenge of uncertainty in production scheduling. For instance, Chang et al. (2010), Liu et al. (2016), and Xiang et al. (2018) introduced a rolling time window rescheduling method to continuously adjust future schedules during the execution of berth allocation and QC assignment and scheduling plans. When dealing with the QCSP, Dik and Kozan (2017), Rouky et al. (2019), and Zhang et al., (2020b) developed robust scheduling plans capable of withstanding operation time fluctuations to a certain extent. In the case of the QC, IV, and YC integrated scheduling problem, Zhang and Jiang (2008), Cahyono et al. (2022), and Ahmed et al. (2021) devised real-time task dispatching rules to dynamically assign tasks instead of generating a global schedule. These methods correspond to predictive-reactive scheduling (PRS), robust-proactive scheduling (RPS), and completely-reactive scheduling (CRS) approaches, respectively (Cai et al., 2023b, 2022; Yang et al., 2024). Predictive-reactive scheduling, which requires frequent rescheduling, suffers from poor real-time performance due to the time-consuming schedule generation process. Completely-reactive scheduling, although more computationally efficient and flexible, is limited to local optimization and lacks the ability to generate a global optimal schedule. Both CRS and RPS are reactive scheduling approaches triggered by specific events or conditions, allowing for the generation of new schedules or modifications to the existing schedule. The key distinction lies in the scheduling window, with CRS having a narrower focus on local scheduling. Given their characteristics, CRS and RPS are better suited for addressing emergency or unforeseen events, such as sudden equipment failures. Robust-proactive scheduling incorporates uncertainty analysis to formulate a robust schedule with a certain level of predictability. As this paper primarily concerns the uncertainty of operation time fluctuations,

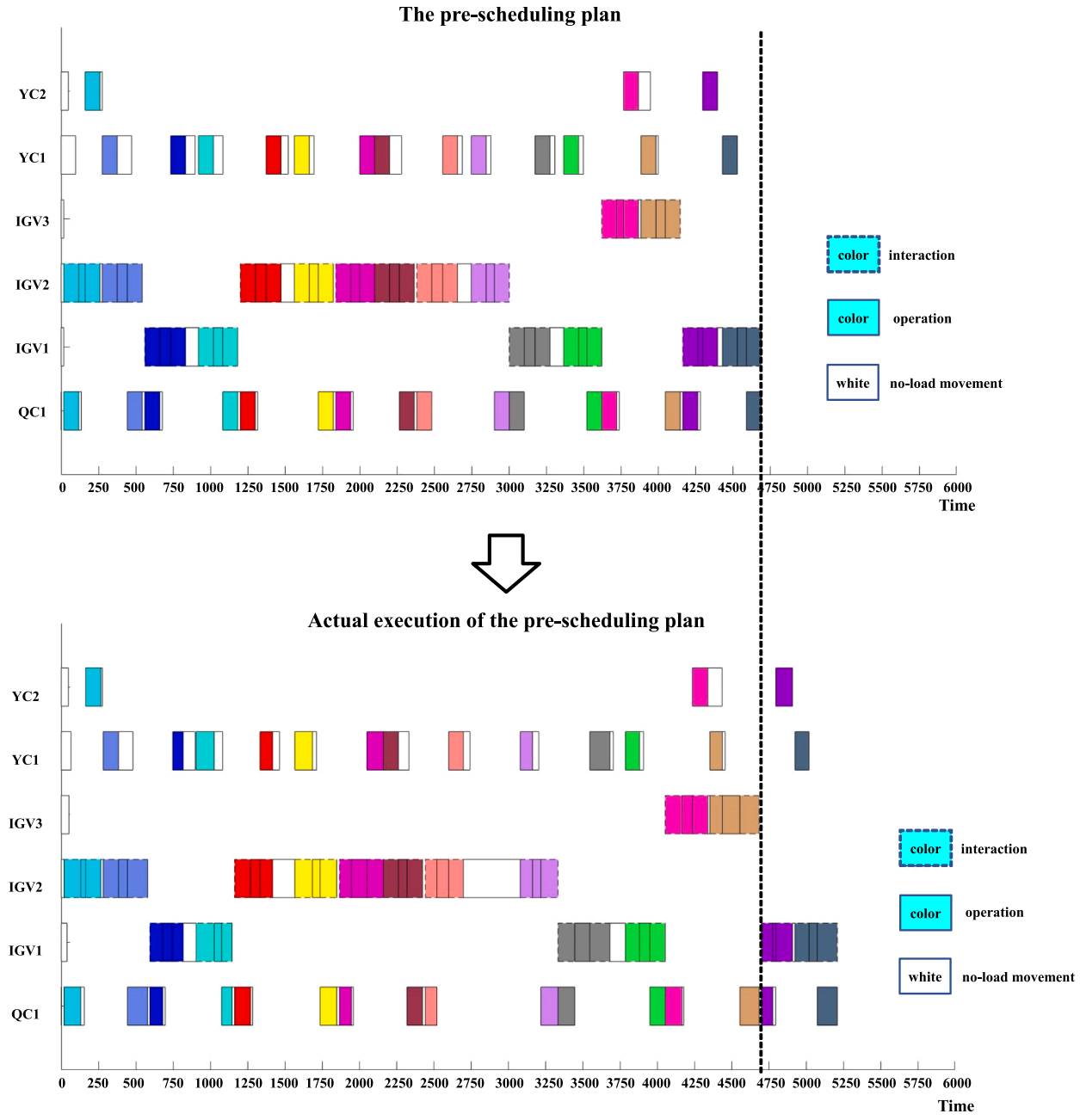

Fig. 3. Scheduling plans with operational time fluctuations.

which exhibit a certain regularity and can be analyzed for generating robust and proactive schedules, its main focus is on the RPS.

This paper aims to develop a new scheduling method to effectively address the gap time slots between operations in the schedules (as demonstrated in Fig. 3), as it has been identified as a key factor influencing schedule robustness in the current literature (e.g. Cai et al., 2023a) and the new solution will improve scheduling and generate significant economic benefits. It is argued that when two scheduling plans have similar *makespans*, the plan with a higher number of gap times slots and a more evenly distributed allocation of these gap times slots may be preferable. The slots of gap time are viewed as buffers to absorb uncertain fluctuations in operation time during schedule execution. Besides, the evaluation of the weight of each gap time slot should also take into account the uncertainty degree of the operation time in the vicinity of the gap time slot. If the time for a specific operation is more volatile, then the adjacent gap time slots should be considered more critical and assigned higher weights. Based on this concept and as a solution to this issue, the scheduling plan is treated as a complex network, and a novel evaluation mechanism based on complex network structure entropy is proposed to assess the robustness and anti-cascade effects of the scheduling plan. By combining this evaluation index with the

Table 1
Review of the integrated scheduling involving QCs, IVs and YCs.

Article	The layout of the container terminal	Where can IVs interact with YCs?	Uncertain factors	Is the cascade effect of uncertainty considered?	Approaches to address uncertainty	Is double-cycling considered?	Models and methods	Case study
Zhang and Jiang, 2008	?	?	General disturbance	×	CRS	×	DES−>DR	Container terminal in *China*
Zeng and Yang, 2009	?	?	Uncertain operation time	×	RPS	×	MIP−>(DR + GA + NN)−>DES	?
Chen et al., 2013	?	?	×	×	×	√	CP−>MHA	?
Lu and Le, 2014	Parallel yard	Loading/Unloading point next to the bay	Uncertain operation time	×	RPS	×	MIP−>PSO	Container terminal in *China*
Xin et al., 2014	Perpendicular yard	AGV mate/buffer at the end of the yard	×	×	×	×	DED(MIP + Cplex) + CTD	?
He et al., 2015	Parallel yard	Loading/Unloading point next to the bay	×	×	×	√	MIP−>(GA + PSO)	?
Xin et al., 2015	Perpendicular yard	The delivery point at the end of the yard	×	×	×	×	MIP−>VNSMA	?
Yang et al., 2018	Perpendicular yard	AGV mate/buffer at the end of the yard	×	×	×	√	Two-level MIP−>Improved GA	?
Zhong et al., 2019	Perpendicular yard	AGV mate/buffer at the end of the yard	×	×	×	√	MIP−>(GA + PSO)	?
Kizilay et al., 2020	?	?	×	×	×	×	CP−>HA	Container terminal in *Turkey*
Cahyono et al., 2022	Perpendicular yard	The delivery point at the end of the yard	General disturbance	×	CRS	√	DES(MPA)	Container terminal in *Indonesia*
Luan et al., 2021	?	AGV mate/buffer at the end of the yard	×	×	×	√	MIP(STN)−>(CRR + GA + TSA)	?
Ahmed et al., 2021	?	?	Uncertain operation time	×	CRS	√	DES	Real container terminal
Hsu et al., 2021a,b	?	?	×	×	×	×	MIP−>Improved PSO	?
Xu et al., 2021	U-shape	Loading/Unloading point next to the bay	×	×	×	√	MIP−>GA(RL)	?
Xu et al., 2022	U-shape	Loading/Unloading point next to the bay	×	×	×	×	MIP−>GSOA	?
Niu et al., 2022	U-shape	Loading/Unloading point next to the bay	×	×	×	√	MIP−>DT(MCTS)	Container terminal in *China*
Zhuang et al., 2022	Perpendicular yard	AGV mate/buffer at the end of the yard	×	×	×	√	MIP−>ALNS	Container terminal in *China*
Zhang et al., 2022a	?	?	×	×	√	×	CQN	Container terminal in *China*
Cai et al., 2023a	?	Loading/Unloading point next to the bay	Uncertain operation time	√	RPS	×	MIP−>GA−>AERI	?
This paper	U-shape	Loading/Unloading point next to the bay	Uncertain operation time	√	RPS	√	Bi-objectives MIP−>NSGA-II(AERI)	Container terminal in *China*

AERI: Anti-cascade Effect and Robustness Index. ALNS: Adaptive Large Neighborhood Search Algorithm. CP: Constraint Programming. CRR: Conflict Resolution Rule. CRS: Completely-Reactive Scheduling. CQN: Closed Queuing Network. CTD: Continuous Time Dynamics. DED: Discrete Event Dynamics. DES: Discrete Event Simulation. DR: Dispatching Rule. DT: Decision Tree. GA: Genetic Algorithm. GSOA: Genetic Seagull Optimization Algorithm. HA: Heuristic Algorithms. MAS: Multi-Agent Simulation. MCTS: Monte Carlo Tree Search. MHA: Meta-Heuristic Algorithm. MIP: Mixed-Integer Programming. MPA: Model Predictive Algorithm. NN: Neural Network. NSGA-II: Non-dominated Sorting Genetic Algorithm-II. PSO: Particle Swarm Optimization. RL: Reinforcement Learning. RPS: Robust-Proactive Scheduling. STN: Space-Time Network. TSA: Tabu Search Algorithm. VNSMA: Variable Neighborhood Search Metaheuristic algorithm. "?": Unknown. "−>": Progressive Relation. "+": Coordinate Relation. "( )": Inclusion Relation or Priority .

makespan, a bi-objective optimization problem is formulated to optimize the scheduling plan.

The remainder of this study is organized as follows: Section 2 discusses the relevant literature to highlight the novelty and significance of our research. Section 3 illustrates the newly proposed RPS framework, outlining the general approach to solving the integrated scheduling problem. Section 4 describes a mixed integer programming model for the integrated scheduling problem of QCs, IGVs, and YCs under the double-cycling mode in a U-shaped container terminal. Section 5 introduces the robustness and anti-cascade effect index designed in this paper. Section 6 presents our experimental results and provides a discussion of the findings. Finally, Section 7 provides practical implications derived from the study, along with the conclusion and future research prospects.

2. Related work

Table 1 summaries a comprehensive review of the literature published in relevant journals pertaining to the integrated scheduling of QCs, IVs, and YCs in port settings. Overall, while this problem has gained attention as a research hotspot, there is a noticeable scarcity of associated research studies that explicitly address the challenges of uncertainty in scheduling.

Approximately 30 % of the existing literature focused on scenarios with a perpendicular yard layout, 10 % focused on a parallel layout, 15 % focused on a U-shaped layout, and 45 % did not mention the port layout. It can be seen that the majority of the literature mentioned the port layout. The majority of the literature focused on scenarios with a perpendicular yard layout, often incorporating an AGV mate as an automated container transfer platform. This device serves as an auxiliary for AGVs, reducing waiting time between YCs and AGVs and providing container buffering capabilities. By disregarding the mutual waiting time between AGVs and YCs, the development of the mathematical model for the scheduling problem becomes simplified. However, this scenario's drawback lies in the increased energy consumption due to the movement of YCs from their current positions to the end of the yard. On the other hand, in yard with parallel or U-shaped layouts, IVs offer greater flexibility, enabling them to penetrate deep into the yard and interact directly with YCs. It results in more energy-efficient operations, although it also introduces scheduling complexities.

Furthermore, a significant observation from the literature is the increasing consideration of double-cycling, highlighting its growing applications. This observation underscores the growing adoption of the double-cycling operation in real-world ports, which justifies the necessity and also stimulate the incorporation of the double-cycling mode in this paper.

To facilitate the discussion, the characteristics of the related research are presented from two perspectives: static integrated scheduling and dynamic integrated scheduling concerning uncertainty in the ensuing sections.

2.1. Static QCs, IVs, and YCs integrated scheduling problem

From a modeling perspective, the majority of studies in this field have employed mathematical programming models, with the mixed integer programming model being the most commonly used approach, followed by constraint programming (Chen et al., 2013). Some researchers have also developed simulation models. For instance, Zhang et al., (2022a) constructed a queuing theory model for the integrated scheduling of multiple pieces of equipment in a port, assessing various performance indicators such as total handling time, idle rate of QCs, and waiting time of AGVs. To attain a globally optimal solution to the greatest extent possible, a mathematical programming model is developed in this paper.

From the perspective of optimization objectives, most studies have focused on optimizing the *makespan* (Hsu et al., 2021b; Xin et al., 2014; Yang et al., 2018; Zhong et al., 2019; Zhuang et al., 2022) or other time-related indicators. A smaller number of studies have considered energy consumption (He et al., 2015; Xin et al., 2014). For example, Xin et al. (2014) proposed a scheduling method based on a two-layer dynamics approach, where the DED in the upper layer optimized the *makespan*, while the CTD in the lower layer optimized energy consumption. He et al. (2015) optimized two objectives: the total vessel departure delay and the total energy consumption. They employed a linear weighting method to convert the two objectives into a single objective and designed a GA for global search and a PSO algorithm for local search. In this study, the focus is placed on both the robustness of the scheduling plan and the minimization of the *makespan* as our primary optimization objectives.

On the one hand, the problem was simplified in certain studies. For instance, only one QC is involved in Xin et al. (2014). To address this limitation, subsequent research by Xin et al. (2015) focused on multiple QCs. However, the subsequent study did not specifically take into account the no-load movement time of YC and instead replaced it with a fixed reserved time. Similarly, Kizilay et al. (2020) disregarded the empty traveling time for the IVs to reduce the complexity of the problem.

On the other hand, more detailed considerations were made in some studies, with a particular focus on the planning of routes for IVs and the resolution of conflicts. For instance, Xin et al. (2015) took into account collision-free trajectories for AGVs. Yang et al. (2018) developed a congestion prevention rule-based bi-level GA to address the route planning problem of AGVs. Luan et al. (2021) investigated conflict-free route planning for AGVs, utilizing an STN representation method and a bi-level optimization algorithm for conflict resolution. Within this context, the route conflicts of IVs are addressed in our study by taking into account the fact that the fluctuations in the travel time of IVs are caused by factors such as collisions in their routes.

There is a research trend to further incorporate additional factors into the integrated scheduling problem of QCs, IVs, and YCs to better reflect the practical needs. Kizilay et al. (2020) considered the assignment problem of QC, YC, and yard space based on the original problem, albeit simplifying the complexity by neglecting the no-load transportation time of IVs. Hsu et al. (2021b) investigated the integrated scheduling and allocation problem involving QCs, YCs, IVs, vessel stowage, and yard space. However, the integration of an increased number of elements into the schedule will potentially compromise its robustness and increase computational complexity. Therefore, the focus of this study seeks a solution to striking a balance between optimization and robustness in the process of integrating QCs, IVs, and YCs.

As discussed in Section 1, the integrated scheduling problem of multiple-equipment in ports can be categorized as a hybrid flow-shop scheduling problem. Consequently, several studies have simplified this problem by abstracting it into a general production scheduling model. For instance, Xin et al. (2014) approached the integrated scheduling problem of QCs, IVs, and YCs as a three-stage flow-shop problem. Taking into account the limited buffer constraints in AGV mate and the double-cycling operation mode, Zhuang et al. (2022) further abstracted this problem into a blocking hybrid flow-shop scheduling problem with bi-directional flows and limited buffers. In line with these approaches, the problem under investigation in this paper can be abstracted as a three-stage hybrid flow-shop scheduling problem with bidirectional flows and waiting time, while also concerning the uncertainty in operation time and its cascade effects.

Lastly, it is worth noting that the integrated scheduling problem for multi-equipment in a U-shaped port has received considerable attention from researchers in recent years. Xu et al., (2022, 2021) addressed the integrated scheduling problem of QCs, conflict-free AGVs, and YCs in a U-shaped port, considering both with and without the consideration of double-cycling operation, respectively. Niu et al. (2022) extended the scope by incorporating EVs into the U-shaped port integrated scheduling model and emphasizing energy consumption in port operations. However, these works failed to incorporate the uncertain operation time and its cascade effects, revealing their limited contributions to practical solutions and the need to develop new solutions to the problem.

2.2. Dynamic QCs, IVs, and YCs integrated scheduling problem concerning uncertainty

In general, there are limited studies that specifically address uncertainty in the context of integrated scheduling. Some studies have introduced general disturbances or uncertainties into DESs without specifying the types of uncertainty. For instance, Zhang and Jiang (2008) incorporated disturbances into the *WITNESS* simulation and evaluated the effectiveness of proposed DRs in improving the operating efficiency of container terminals. Similarly, Cahyono et al. (2022) considered general disturbances and integrated a HA into a DES to obtain near-optimal solutions.

Other studies have specifically focused on uncertain operation time. For instance, Zeng and Yang (2009) assumed that the operation time of QCs and YCs followed a *Uniform* distribution and investigated the scheduling problem for outbound containers as a hybrid flow shop scheduling problem. They employed a GA to optimize the initial schedule generated by DRs and utilized simulation to evaluate the effectiveness of the schedule. Notably, they developed a surrogate model based on a NN to quickly predict the value of the fitness function. However, their study did not account for the fluctuation of IVs' transportation time, while our research takes this factor into consideration.

Ahmed et al. (2021), Cai et al., (2023a), and Lu and Le (2014) tackled the issue of uncertain operation time for IVs, and cranes. Lu and Le (2014) specifically optimized the operation time of YCs in coordination with QCs and ITs. However, their approach employed a PSO algorithm that substituted deterministic parameters with randomly generated parameters following a normal distribution, without sufficiently delving into an extensive analysis of the uncertainty-solving mechanism. Additionally, it is worth noting that they did not consider the double-cycling operation mode and U-shaped layout in their studies, whereas our study has specifically addressed this aspect. Ahmed et al. (2021) investigated the double-cycling operation mode, which was highly relevant to the problem addressed in our paper. Nevertheless, their study adopted a CRS approach and primarily focused on comparing the productivity rate, vessel turnaround time, and unit cost of double-cycling and single-cycling strategies, rather than placing emphasis on global optimization and schedule robustness, as we have done in this paper. Besides, the U-shaped layout was not considered in their work, whereas it is considered in this work. The study by Cai et al., (2023a) has not yet considered the U-shaped port layout and the double-cycling operation, requiring new exploration to make the new theoretical development best-fit the increasing practical needs in this field. Besides, in terms of the scale of their experimental case, it is evident that the current literature has not conducted the experiments to a large scale that can match reality and fully validate the feasibility of the new models in practice. Methodologically, this paper provides a new robust scheduling plan generation framework based on such scheduling plan's robustness and AERI which is transforming this index into an optimization objective and transforming the original problem into a multi-objective optimization problem.

2.3. Research gaps and our contribution

Compared to the existing literature, this paper makes four significant contributions (i.e., **C1-C4**) to the field to fill the research gaps (i.e. **R1-R4**):

R1: The simultaneous consideration of uncertain operation time, U-shaped port layout, and double-cycling mode in solving the integrated scheduling of QCs, IGVs, and YCs has not been addressed in prior research.

C1: A new scheduling solution to the coordination of QCs, IGVs, and YCs in a U-shaped port terminal concerning uncertain operation time and its cascade effects under the double-cycling mode.

Uncertain operation times are a frequent phenomenon in real-world port operations, and it is yet fully explored in integrated scheduling research. Furthermore, the U-shaped layout and double-cycling operation mode, which offer enhanced efficiency and energy savings, require a tailored scheduling approach to optimize the port's container handling capacity. Consequently, the significance of this study lies in its ability to address a critical issue in the port industry and cater to the trend of a more efficient industrial mode.

R2: Given the aforementioned challenges, the existing methods for addressing uncertain operation time seldom focus on the cascade effects of operation time fluctuations, upon which a more effective scheduling method can be developed.

C2: A new robust-proactive scheduling framework concerning scheduling plans' robustness and anti-cascade effect based on complex network structure entropy.

The significance of this new robust-proactive scheduling framework lies in its proactive approach to scheduling, which takes into account the potential cascading effects of disruptions in the schedule. By incorporating the concept of complex network structure entropy, the framework provides a method for evaluating the robustness of scheduling plans and mitigating the impact of critical components that may lead to cascading failures to a certain extent. This approach holds applicability not only in the multi-equipment integrated scheduling but also in other complex scheduling systems, including workshop production scheduling, warehouse AGVs scheduling and transportation vehicle scheduling, among others.

R3: Only a limited number of studies have utilized real port cases.

C3: A real case study upscaling the experiment size to best-fit the reality to demonstrate the feasibility of the new method and the supporting mathematic formulation and algorithms in the real world.

The experimental parameters and port layout used in this study are derived from a comprehensive survey of real ports. The real-case study can help demonstrate the feasibility of the proposed method and validate the effectiveness of the mathematical formulation and algorithms in practical settings, which holds significant value. Future application of this method to a real-world port terminal will provide valuable insights into its performance and identify areas for further enhancement. Moreover, the case study can serve as a reference for other ports or logistics companies interested in implementing the new method.

R4: The implications of their research for the industry are mentioned less frequently in existing studies.

C4: Elaboration of the new method's implications and significance in the port industry or other sectors facing similar problems.

The cross-industry applicability of the new method is a notable feature. Its capacity to handle uncertain and dynamic situations, optimize complex scheduling systems, and consider the cascading effects of disruptions makes it valuable for other industries such as workshop production logistics scheduling, warehouse logistics AGVs scheduling and city logistics vehicles scheduling. These industries

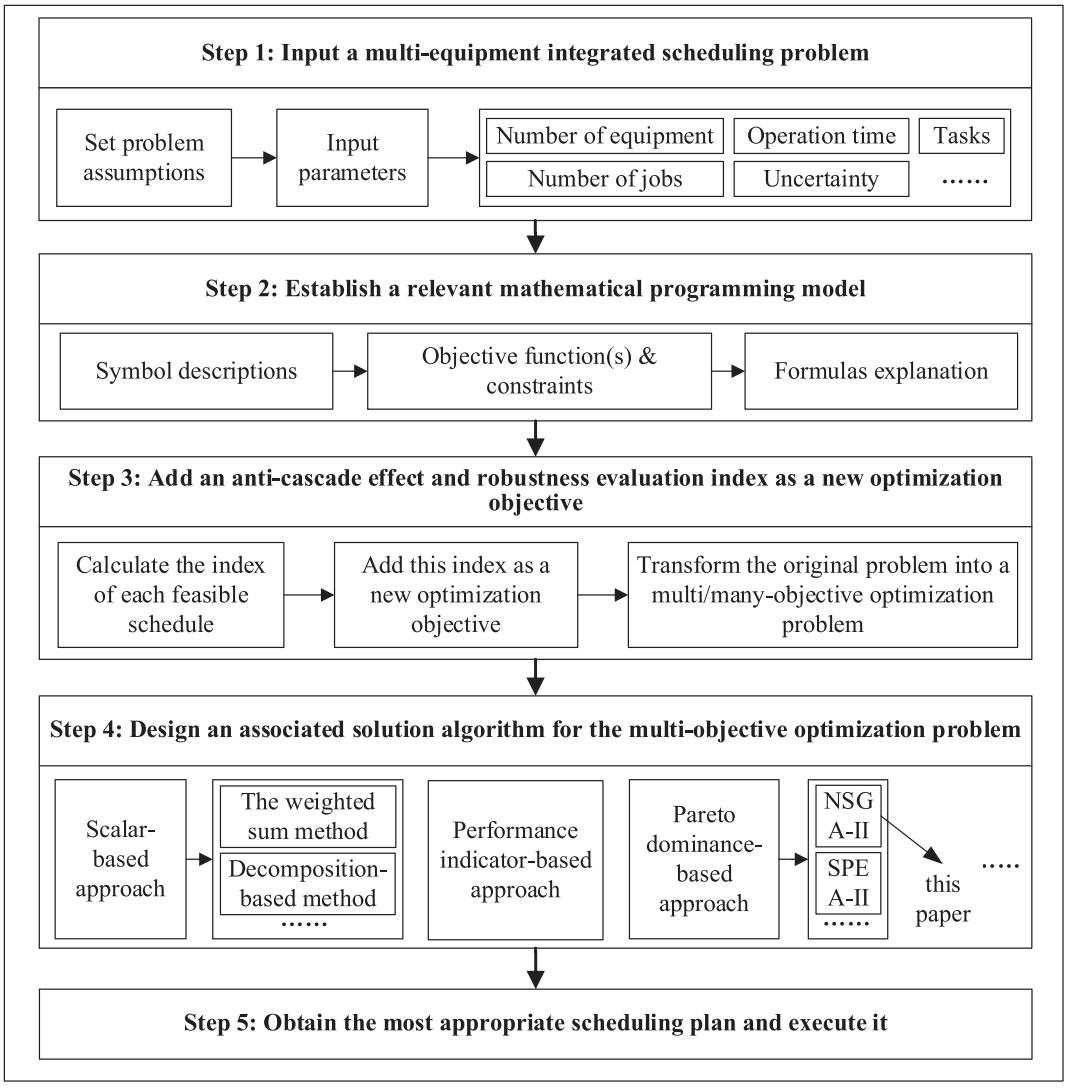

Fig. 4. A robust-proactive scheduling framework.

face similar challenges and can benefit from the application of the newly proposed method in this paper.

3. The proposed robust-proactive scheduling framework

This section outlines the development of the proposed robust-proactive scheduling framework. Fig. 4 illustrates the approach used to address the port multi-equipment integrated scheduling problem while concerning uncertainty with cascade effects. Additionally, it shows how the designed anti-cascade effect and robustness evaluation index are applied to feasible scheduling plans. The framework incorporates this index as an additional optimization objective in the original problem, effectively transforming it into a multi-objective optimization problem (Zhu et al., 2018).

The approaches to solving multi-objective optimization problems can be classified into three categories: scalar-based, performance-based, and Pareto dominance-based (He et al., 2019b). The scalar-based approaches include those like weighted sum (Kaddani et al., 2017) and decomposition-based (Jiang et al., 2021; Zhang et al., 2020a) methods, which are easy to implement but may have challenges in determining the weight values for each objective (He et al., 2022). The performance indicator-based approaches are less commonly used compared to the other two. It involves using indicators such as hypervolume, inverted generational distance, and generational distance to evaluate the quality of each solution and using these indicators as objective functions in evolutionary algorithms. While this type of approach can accurately measure solution quality and handle objective interactions and solution set control, it may not align well with an actual problem, and the computational complexity can be high (Kaveh et al., 2012). The Pareto dominance-based approaches are widely popular, with Nondominated Sorting Genetic Algorithm II (NSGA-II) (Ming et al., 2022) and Strength Pareto Evolutionary Algorithm II (SPEA-II) (Yuan et al., 2017) being the most commonly used methods in this domain. This type of approach is effective but may be time-consuming in terms of computation. In this paper, the main focus is placed more on obtaining a robust scheduling plan than a multi-objective optimization algorithm itself. Therefore, the widely used and effective NSGA-

Table 2
Notations used in the mathematic formulation model.

Notation	Description	Notation	Description
***Sets* and *indices*:**			
C_I	Set of the serial number of inbound containers.$C_I = \{1, \cdots\cdots, N_I\}$.	C_O	Set of the serial number of outbound containers.$C_O = \{N_I+1, \cdots\cdots, N_I+N_O\}$.
C	Set of all the serial number of containers. $C = C_I \cup C_O$	J	Set of the serial number of operations that a container needs to go through. $J = \{1,2,3\}$.
Q	Set of the serial number of QCs. $Q = \{1, \cdots\cdots, N_Q\}$.	A	Set of the serial number of IGVs. $A = \{N_Q+1, \cdots\cdots, N_Q+N_A\}$.
Y	Set of the serial number of YCs. $Y = \{N_Q+N_A+1, \cdots\cdots, N_Q+N_A+N_Y\}$.	K	Set of the serial number of equipment. K=$Q \cup A \cup Y$
i,i'	Index for containers. When $i,i' \in C_I$, they refer to an inbound container. When $i,i' \in C_O$, they refer to an outbound container.	j	Index for operations that a container needs to go through. $j = 1, 2, 3$ refer to the unloading operation from the vessel, the transportation operation, and the loading operation onto the yard respectively.
k	Index for equipment. When $k \in Q$, k refers to a QC. When $k \in A$, k refers to an AGV. When $k \in Y$, k refers to a YC.		
***Parameters*:**			
N_I	The total number of inbound containers to be handled. $N_I = N_O$.	N_O	The total number of outbound containers to be handled. $N_I = N_O$.
N_Q	The total number of QCs.	N_A	The total number of AGVs.
N_Y	The total number of YCs.	O_{ij}	The jth operation of container i.
$\widetilde{t}_{ij}$	The loading, unloading or transportation time of operation O_{ij}.	H	An exceptionally high positive integer.
$\widetilde{v}_k$	The movement speed of the kth equipment.	$D_{ii'k}$	The distance that equipment k needs to travel between the ending position of operation O_{ij} and the starting position of operation $O_{i'j}$. The value of j depends on the type of equipment, where j takes values of 1, 2 or 3, respectively when $k \in Q, A$ or Y, respectively.
M_i	The index of the QC responsible for handling container i.	G_i	The index of the YC responsible for handling container i.
***0–1 variables*:**			
x_{ik}	1 if O_{ij} is assigned to the equipment k and 0 otherwise. The value of j depends on the type of equipment, where j takes values of 1, 2 or 3, respectively when $k \in Q, A$ or Y, respectively.	$y_{ii'k}$	1 if O_{ij} precedes $O_{i'j}$ and 0 otherwise. The value of j depends on the type of equipment, where j takes values of 1, 2 or 3, respectively when $k \in Q, A$ or Y, respectively.
$P_{ii'}$	1 if an inbound container $i \in C_I$ can form a pair with an outbound container $i' \in C_O$ and 0 otherwise. In a pair, the IGA operates in a double-cycling mode, where it will promptly proceed to transport the outbound container as soon as it completes the transportation of the corresponding inbound co/ntainer in the pair.	$u_{1ii'}$, u_{2ik}	Auxiliary variables used to linearize constraints.
***Non 0–1 variables*:**			
C_{max}	The *makespan* which is the time when all the operations are finished.	St_{ij}	The start time of operation O_{ij}.

II algorithm has been chosen to solve the multi-objective mathematical programming model presented in this study.

This framework serves as a general approach to address the scheduling problem with uncertain operation time. By utilizing this framework, the generated scheduling plan not only improves the original optimization objective, such as *makespan*, but also maintains a high level of robustness when facing actual uncertain operation time. In particular, the framework can effectively absorb a certain degree of operation time fluctuations. Hence, the proposed framework is in naturally categorized as an improvement under the Robust-Proactive Scheduling (RPS) approach.

4. Preliminary

The integrated scheduling of QCs, IVs, and YCs in a U-shaped container terminal, taking into account uncertain operation time and the double-cycling mode, is formulated as a three-stage hybrid flow shop scheduling problem with bi-directional flows, waiting time, and uncertain operation time, as analyzed above. This section describes the detailed development of a new mathematical model for the formulated problem. The basic model primarily focuses on optimizing the *makespan*. However, in the subsequent section, an additional optimization objective related to robustness and anti-cascade effect is also introduced.

4.1. Problem assumptions

Before presenting the mathematical formulation model, the following assumptions are outlined:

1) All equipment, including QCs, IGVs, and YCs, are available at the start of the scheduling process.
2) All tasks, including loading outbound containers from an investigated yard to a vessel and unloading inbound containers from the vessel to the yard, are available at the start, following the double-cycling mode. Each IGV can transport inbound and outbound containers alternatively as required.
3) Each equipment can handle only one container at a time, performing operations such as loading, unloading, or transportation.
4) Each container can be handled by only one equipment at a time, whether it's for loading, unloading, or transportation purposes.
5) The assignment of QCs and YCs is predetermined.
6) The layout of the U-shaped port container terminal, including the distance between the two loading and unloading positions, is known and predefined. As such, the traveling distances matrix for IGVs between each unloading/loading point is ascertainable.
7) The IGVs are shared among all QCs and YCs, enabling each IGV to serve multiple QCs and YCs.
8) The average loading or unloading time of a QC or YC, as well as the horizontal moving speed of a QC, IGV, or YC, are known based on historical data.
9) The actual loading or unloading time of a QC or YC, as well as the horizontal moving speed of a QC, IGV, or YC, may fluctuate around the average time due to uncertainties such as human operation, traffic congestion, weather changes, equipment obstacle avoidance, and failures, among others.

4.2. Basic mixed-integer programming model

Table 2 presents the symbols used in the mathematical formulation model.

The objective function of this model is the *makespan*, which is defined as follows:

$Minimize\ f = makespan = C_{max}$ (1).

where Eq. (1) minimizes the maximum completion time of container operations. The constraints of the basic mathematic model are formulated as follows:

$C_{max} \geq St_{i1} + \widetilde{t}_{i1} \forall i \in C_O$(2).

$St_{ij} + \widetilde{t}_{ij} \leq St_{i(j+1)} \forall i \in C_I, j \in \{1,2\}$(3).

$St_{ij} + \widetilde{t}_{ij} \leq St_{i(j-1)} \forall i \in C_O, j \in \{2,3\}$(4).

$St_{ij} - \left(St_{i'(j+1)} + \frac{D_{i'k}}{\widetilde{v}_k} \right) + H\left(2 + y_{ii'k} - x_{ik} - x_{i'k}\right) \geq 0 \forall i \in C, i' \in C_I, j \in \{1\}, k \in Q$(5).

$St_{ij} - \left(St_{i'(j+1)} + \widetilde{t}_{i'(j+1)} + \frac{D_{i'k}}{\widetilde{v}_k} \right) + H\left(2 + y_{ii'k} - x_{ik} - x_{i'k}\right) \geq 0 \forall i \in C, i' \in C_I, j \in \{2\}, k \in A$(6).

$St_{ij} - \left(St_{i'j} + \widetilde{t}_{i'j} + \frac{D_{i'k}}{\widetilde{v}_k} \right) + H\left(2 + y_{ii'k} - x_{ik} - x_{i'k}\right) \geq 0 \forall i \in C, i' \in C_I, j \in \{3\}, k \in Y$(7).

$St_{ij} - \left(St_{i'(j-1)} + \frac{D_{i'k}}{\widetilde{v}_k} \right) + H\left(2 + y_{ii'k} - x_{ik} - x_{i'k}\right) \geq 0 \forall i \in C, i' \in C_O, j \in \{3\}, k \in Y$(8).

$St_{ij} - \left(St_{i'(j-1)} + \widetilde{t}_{i'(j-1)} + \frac{D_{i'k}}{\widetilde{v}_k} \right) + H\left(2 + y_{ii'k} - x_{ik} - x_{i'k}\right) \geq 0 \forall i \in C, i' \in C_O, j \in \{2\}, k \in A$(9).

$St_{ij} - \left(St_{i'j} + \widetilde{t}_{i'j} + \frac{D_{i'k}}{\widetilde{v}_k} \right) + H\left(2 + y_{ii'k} - x_{ik} - x_{i'k}\right) \geq 0 \forall i \in C, i' \in C_O, j \in \{1\}, k \in Q$(10).

$St_{ij} - \left(St_{i(j+1)} + \frac{D_{ik}}{\widetilde{v}_k} \right) + H\left(3 - y_{ii'k} - x_{ik} - x_{i'k}\right) \geq 0 \forall i' \in C, i \in C_I, j \in \{1\}, k \in Q$(11).

$$St_{i'j} - \left(St_{i(j+1)} + \widetilde{t}_{i(j+1)} + \frac{D_{i'ik}}{\widetilde{v}_k} \right) + H\left(3 - y_{i'ik} - x_{ik} - x_{i'k}\right) \geq 0 \forall i' \in C, i \in C_I, j \in \{2\}, k \in A (12).$$

$$St_{i'j} - \left(St_{ij} + \widetilde{t}_{ij} + \frac{D_{i'ik}}{\widetilde{v}_k} \right) + H\left(3 - y_{i'ik} - x_{ik} - x_{i'k}\right) \geq 0 \forall i' \in C, i \in C_I, j \in \{3\}, k \in Y (13).$$

$$St_{i'j} - \left(St_{i(j-1)} + \frac{D_{i'ik}}{\widetilde{v}_k} \right) + H\left(3 - y_{i'ik} - x_{ik} - x_{i'k}\right) \geq 0 \forall i' \in C, i \in C_O, j \in \{3\}, k \in Y (14).$$

$$St_{i'j} - \left(St_{i(j-1)} + \widetilde{t}_{i(j-1)} + \frac{D_{i'ik}}{\widetilde{v}_k} \right) + H\left(3 - y_{i'ik} - x_{ik} - x_{i'k}\right) \geq 0 \forall i' \in C, i \in C_O, j \in \{2\}, k \in A (15).$$

$$St_{i'j} - \left(St_{ij} + \widetilde{t}_{ij} + \frac{D_{i'ik}}{\widetilde{v}_k} \right) + H\left(3 - y_{i'ik} - x_{ik} - x_{i'k}\right) \geq 0 \forall i' \in C, i \in C_O, j \in \{1\}, k \in Q (16).$$

$$P_{ii'} \geq 1 - u_{1_{ii'}} \ \forall i' \in C_O, i \in C_I (17).$$

$$P_{ii'} + x_{ik} + x_{i'k} - 3 + Hu_{1_{ii'}} \geq 0 \forall i' \in C_O, i \in C_I, k \in A (18).$$

$$\sum_{i \in C} y_{i'ik} - \sum_{i' \in C} y_{i'ik} - 1 + Hu_{1_{ii'}} \geq 0 \forall i' \in C_O, i \in C_I, k \in A (19).$$

$$\sum_{i \in C} y_{i'ik} - \sum_{i' \in C} y_{i'ik} - 1 - Hu_{1_{ii'}} \leq 0 \forall i' \in C_O, i \in C_I, k \in A (20).$$

$$x_{iM_i} = 1 \forall i \in C (21).$$

$$x_{iG_i} = 1 \forall i \in C (22).$$

$$\sum_{k \in QorAorY} x_{ik} = 1 \forall i \in C (23).$$

$$\sum_{i' \in C} y_{i'ik} + \sum_{i' \in C} y_{i'ik} - \sum_{i \in C} x_{ik} + 1 - H(1 - u_{2ik}) \leq 0 \forall i \in C, k \in K (24).$$

$$\sum_{i' \in C} y_{i'ik} + \sum_{i' \in C} y_{i'ik} - \sum_{i \in C} x_{ik} + 1 + H(1 - u_{2ik}) \geq 0 \forall i \in C, k \in K (25).$$

$$\sum_{i' \in C} y_{i'ik} + \sum_{i' \in C} y_{i'ik} - \sum_{i \in C} x_{ik} - Hu_{2ik} \leq 0 \forall i \in C, k \in K (26).$$

$$\sum_{i' \in C} y_{i'ik} + \sum_{i' \in C} y_{i'ik} - \sum_{i \in C} x_{ik} + Hu_{2ik} \geq 0 \forall i \in C, k \in K (27).$$

$$\sum_{i \in C} x_{ik} - u_{2ik} \geq 0 \forall i \in C, k \in K (28).$$

$$\sum_{i \in C} x_{ik} - Hu_{2ik} \leq 0 \forall i \in C, k \in K (29).$$

$$\sum_{i' \in C_O} P_{ii'} = 1 \forall i \in C_I (30).$$

$$\sum_{i' \in C_I} P_{i'i} = 1 \forall i \in C_O (31).$$

$$\sum_{i \in C_I} \sum_{i' \in C_O} P_{ii'} = N_I = N_O (32).$$

$$x_{ik}, y_{i'ik}, P_{ii'}, u_{1_{ii'}}, u_{2ik} \in \{0,1\} \forall i, i' \in C, k \in K (33).$$

$$St_{ij} \geq 0 \forall i \in C, j \in J (34).$$

Constraint (2) ensures that the *makespan* is not smaller that the completion time of all outbound containers. The final task in an entire scheduling sequence must fall on an outbound container, as an IGV follows a double-cycling order of transporting containers, moving an inbound container and then an outbound container in a sequential manner. Constraints (3) to (4) enforce that the start time of a subsequent operation cannot be earlier than the completion time of its preceding operation. Constraints (5) to (16) establish the sequential relationships between two containers assigned to the same equipment. Constraints (17) to (20) are linearized versions of the constraints $P_{ii'}(x_{ik} + x_{i'k} - 2) = 0 \forall i \in C_I, i' \in C_O, k \in A$ and $P_{ii'}\left(\sum_{i \in C} y_{i'ik} - \sum_{i' \in C} y_{i'ik} - 1\right) = 0 \ \forall i \in C_I, i' \in C_O, k \in A$. These constraints impose the condition that the IGV must transport inbound and outbound containers alternately, representing a double-cycling operation mode. Constraint (21) indicates that QCs are assigned to their respective containers based on a predetermined plan that considers collision avoidance between QCs. Constraint (22) specifies the assignment of YCs to their respective containers while avoiding collisions between YCs. Constraint (23) ensures that each container operation is assigned to only one equipment of the same type, meaning that multiple equipment of the same type cannot simultaneously perform the operation on the same container. Constraints (24) to (29) linearize the constraint $\sum_{i' \in C} y_{i'ik} + \sum_{i' \in C} y_{i'ik} = \begin{cases} \sum_{i \in C} x_{ik} - 1, if \sum_{i \in C} x_{ik} \neq 0 \\ 0, if \sum_{i \in C} x_{ik} = 0 \end{cases} \forall i \in C, k \in K$, establishing the relationship between assignment variables and operation sequence variables for a piece of equipment. Constraints (30) to (31) indicate that each inbound container can only be paired with one outbound container, and each outbound container can only be paired with one inbound container, forming a double-cycling pattern. Constraint (32) ensures that every container is paired. Constraints (33) to (34) define the value range of the variables.

5. Bi-objective optimization model concerning the anti-cascade effect and robustness evaluation index

5.1. Bi-objective robust optimization model

Using the basic mathematical model with a single optimization objective as a foundation, a bi-objective robust optimization model is developed by incorporating an additional objective to evaluate the robustness of a pre-scheduling plan. This approach aims to obtain a Pareto frontier consisting of solutions that exhibit both good *makespans* and strong robustness against cascade effects ability.

If S represents a feasible pre-scheduling plan, which is determined by the variables and constraints outlined in Section 4.2 of the basic mathematical model, the original objective function can be reformulated as Eqs. (35) - (37):

$$f(S) = Minimize[f_1(S), f_2(S)] (35).$$

$$f_1 = Makespan(S) (36).$$

$$f_2 = -R(S) (37).$$

where f_1 represents the *makespan*, as mentioned previously, and f_2 indicates the anti-cascade effect and robustness evaluation index with regard to the schedule.

5.2. Anti-cascade effect and robustness evaluation index based on complex network structure entropy

5.2.1. Gap time slots between consecutive operations

During the implementation of the schedule, uncertainties may arise, leading to fluctuations in operation time. While the fluctuation of a single operation may have minimal impact on that particular operation, the interdependence between operations can result in cascade effects when multiple operation time fluctuations occur. These cascade effects can propagate throughout the original scheduling plan, rendering it ineffective. Therefore, it is crucial to generate a robust pre-scheduling plan that can absorb operation time fluctuations during execution. One of the objectives of this paper is to develop a mechanism to evaluate the anti-cascade effect and robustness of schedules. This mechanism will aid in selecting a more suitable scheduling plan for implementation.

In the Gantt Charts of the pre-scheduling plans, noticeable gap time slots are often observed between operations. A gap time slot refers to the duration between two consecutive operations within an equipment or job. It represents the idle time between tasks. The development of the anti-cascade effect and robustness evaluation mechanism for pre-scheduling plans involves analyzing the size and distribution of these gap time slots in the Gantt Charts. Having more gap time slots between operations indicates a greater ability of the pre-scheduling plan to absorb uncertainties. However, it is not only the total length of these gap time slots that matters but also their distribution that is important.

For example, two sets of comparisons regarding gap time slots are provided in Fig. 5. In Fig. 5(a), it can be observed that scheduling plan 1 has a better *makespan* than scheduling plan 2, but it lacks any gap time slot between operations. Consequently, when facing operation time fluctuations during plan execution, scheduling plan 2 will exhibit greater robustness compared to scheduling plan 1. However, it is important to note that having more gap time slots does not automatically indicate a superior scheduling plan. As illustrated in Fig. 5(b), even though scheduling plan 4 has a larger total length of gap time slots than scheduling plan 3, the gap time slots in scheduling plan 3 are more evenly distributed. Therefore, concerning the cascade effects of uncertain operation time slots, scheduling plan 4 is expected to possess a greater capacity to absorb uncertainties at a higher level compared to scheduling plan 3.

5.2.2. The construction of anti-cascade effect and robustness evaluation index

In complex network theory, a metric known as complex network structure entropy is employed to measure the complexity of a network (Fu et al., 2023; Lei et al., 2019). An illustration of this concept is depicted in Fig. 6. The network depicted on the left, which appears more intricate and uniform, exhibits a higher level of network structure entropy compared to the one on the right. Consequently, the network on the left demonstrates a greater degree of resilience, suggesting that it is more likely to remain operational and avoid complete failure in the face of node failures and their cascade effects. Specifically, the failure of one node in Fig. 6(a) does not incapacitate the entire system since alternative routes exist through other connections. Conversely, the failure of the central node in Fig. 6(b) can trigger a cascading effect that results in a system-wide failure. To quantify this anti-cascade effect and robustness, the theory of complex network structure entropy has been employed here.

As previously expounded, a schedule's robustness and anti-cascade effect directly correlate with the uniform distribution and greater lengths of gap time slots between operations. In such circumstances, the capacity of gap time slots to absorb uncertainty is enhanced, bolstering the schedule's anti-cascade effect and robustness. This implies a certain correlation between gap time slots and the nodes and connections within a complex network. The fundamental concept underlying the application of this theory to scheduling is to transform the scheduling plan into a complex network, making it amenable to complex network theory analysis. Furthermore, it necessitates the incorporation of the significance and priority of operations with respect to uncertainty, achieved by devising a function reflecting the weight of each gap time slot's importance.

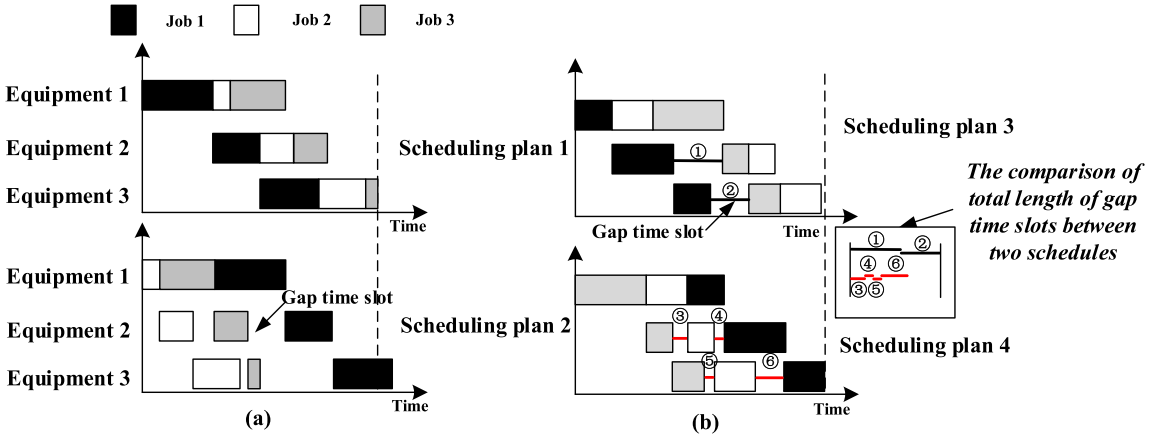

Fig. 5. The comparison of gap time slots among different pre-scheduling plans.

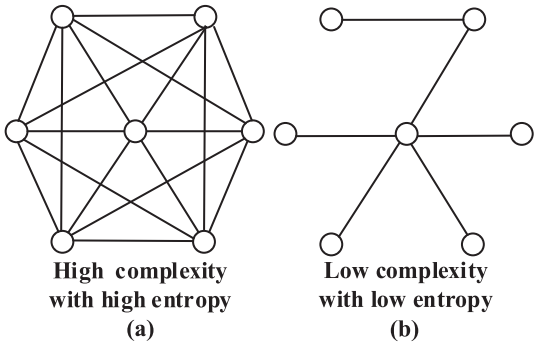

Fig. 6. Two constructed networks with varying levels of complexity and entropy.

To enhance the application of this theory in evaluating the anti-cascade effects and robustness of a schedule, several steps are undertaken. Initially, the scheduling Gantt Chart is transmuted into a complex structure where operations are represented as nodes connected by solid lines, while gap time slots are denoted by dotted lines. Subsequently, the lengths of the dotted lines on the X-axis, signifying the gap time slots' durations, are calculated. Thirdly, the importance of each dotted line (gap time slot) is computed. In this process, a function is employed to reflect the significance and priority of operations concerning uncertainty. Fourthly, the importance degree of each dotted line is subjected to entropy analysis to quantify the degree of dispersion. Ultimately, the summation of all dispersion degrees of each dotted line represents the network structure entropy or, in other terms, the anti-cascade effect and robustness index of the scheduling plan.

Here are the following steps in detail.

(1) *Preparatory work: Introducing some new notations*.

As presented in Table 3, before introducing the anti-cascade effect and robustness evaluation index of a schedule, it is essential to introduce some additional notations. The uncertain operation time $\widetilde{t}_{ij}$ can be represented in a revised form, as shown in Eq. (38), which includes both the deterministic component and the uncertain component. Furthermore, a random variable ξ_{ij} can be extracted from the uncertain component.

$$\widetilde{t}_{ij} = \left(1+\xi_{ij}\right) \bullet t_{ij} \forall i \in C, j \in J \quad (38).$$

(2) *The first step: Transforming the pre-scheduling plan into a complex network*.

To employ the complex network structure entropy theory for evaluating the anti-cascade effect and robustness, it is necessary to convert the schedule into a network format. A feasible pre-scheduling plan for the operation of three jobs utilizing three pieces of equipment is depicted in Fig. 7. During the transformation process, each operation is depicted by two nodes connected by a directed solid line, while each gap time slot is represented by a dotted line.

(3) *The second step: Calculating the projected length of the dotted line on the X-axis (gap time slot)*.

While the dotted lines visually represent gap time slots, it is important to note that the lengths of the dotted lines do not directly correspond to the durations of the gap time slots. In reality, the lengths of gap time slots are measured as the projected distances of the dotted lines onto the X-axis. The calculation of gap time slots is demonstrated in Fig. 8 using Eqs. (39)-(40).

$$G_{ij} = \begin{cases} St_{i(j+1)} - St_{ij} - t_{ij}, if i \in C_I, j \in \{1,2\} \\ St_{i(j-1)} - St_{ij} - t_{ij}, if i \in C_O, j \in \{2,3\} \end{cases} \quad (39).$$

$$G_{ij}^{k} = \sum_{i \in C} \sum_{k \in K} y_{iik} \bullet \left(St_{ij} - St_{ij} - t_{ij}\right) \forall i \in C, j \in J \quad (40).$$

(4) *The third step: Calculating the importance degree of each dotted line (gap time slot)*.

In the context of complex network structure entropy theory, there exists a concept that describes the importance level of nodes within a network. Specifically, if a node in the network has a higher proportion of connected edges, it possesses a greater degree of importance. This concept can be applied to the scheduling problem. If a gap time slot represents a higher proportion of the total duration of gap time slots, it can be assumed to possess a higher degree of importance. As a result, the importance level of each gap time slot can be defined using Eqs. (44)-(45).

$$N_{G_1} = \sum x_{ij}^{k} - N_{QC} - N_{IGV} - N_{YC} \quad (41).$$

$$N_{G_2} = \sum x_{ij}^{k} - N_I - N_O \quad (42).$$

$$N_G = N_{G_1} + N_{G_2} = 2 \bullet \sum x_{ij}^{k} - \left(N_{QC} + N_{IGV} + N_{YC} + N_C + N_O\right) \quad (43).$$

$$I_{G_{ij}} = \begin{cases} h\left(\xi_{ij}, \xi_{i(j+1)}\right) \bullet \dfrac{G_{ij}}{\sum G_{ij}^{k} + \sum G_{ij}}, if i \in C_I, j \in \{1,2\} \\ h\left(\xi_{ij}, \xi_{i(j-1)}\right) \bullet \dfrac{G_{ij}}{\sum G_{ij}^{k} + \sum G_{ij}}, if i \in C_O, j \in \{2,3\} \end{cases} \quad (44).$$

$$I_{G_{ij}^{k}} = h\left(\xi_{ij}, \xi_{ij}\right) \bullet \frac{G_{ij}^{k}}{\sum G_{ij}^{k} + \sum G_{ij}} where G_{ij}^{k} is between O_{ij} and O_{ij}, \forall i \in C, k \in K \quad (45).$$

It is noteworthy that the model takes into account the influence of the characteristics of uncertainties in adjacent operations. For

Table 3
New notations used in the complex network structure entropy theory.

Notation	Description	Notation	Description
Parameters			
t_{ij}	The deterministic component of operation time $\widetilde{t}_{ij}$.	ξ_{ij}	The random variable describing the uncertain component of operation time $\widetilde{t}_{ij}$.
α	A positive coefficient.		
***Non 0–1 variables*:**			
G_{ij}^{k}	The gap time slot between operation O_{ij} and its subsequent operation in an equipment k.	G_{ij}	The gap time slot between consecutive operations O_{ij} and $O_{i(j+1)}$ in a container i.
N_{G_1}	The cumulative count number of gap time slots between operations in a piece of equipment.	N_{G_2}	The cumulative count number of gap time slots between operations in a container.
N_G	The total number of the gap time slots	$I_{G_{ij}^{k}}, I_{G_{i(j+1)}}$	The importance degree of the gap time slot G_{ij}^{k} or $G_{i(j+1)}$.
$d_{G_{ij}^{k}}, d_{G_{i(j+1)}}$	The dispersion degree of the gap time slot G_{ij}^{k} or $G_{i(j+1)}$		
Function:			
$h()$	A function to manage the random variables of the two operations associated with the gap time slot.		

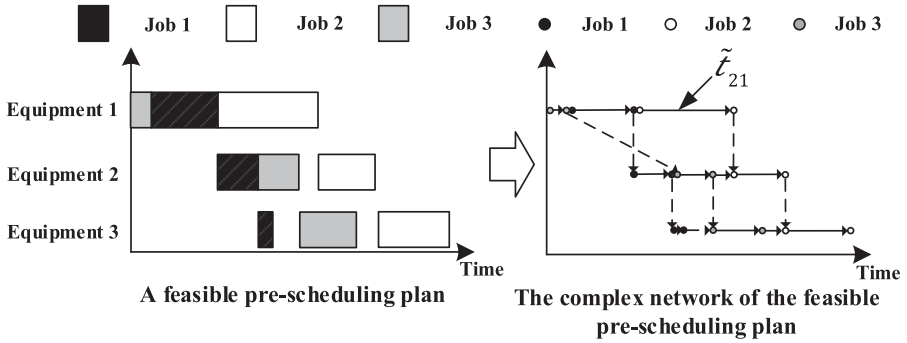

Fig. 7. The approach of transferring the pre-scheduling plan into a network.

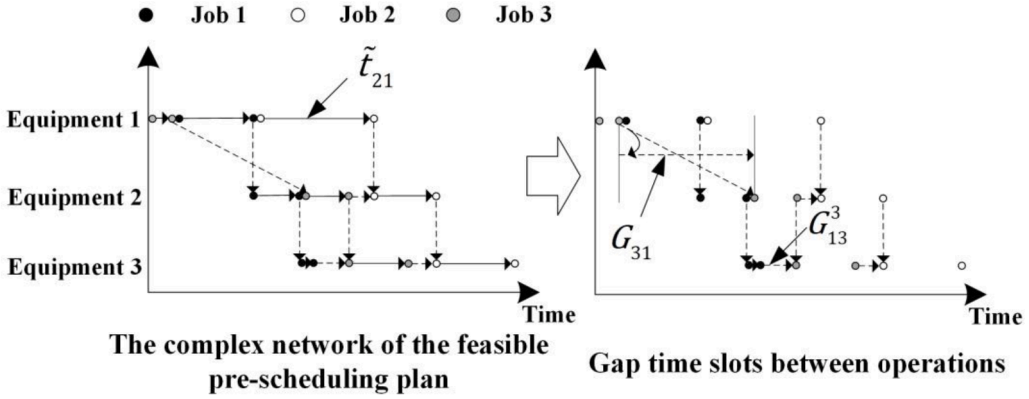

Fig. 8. The gap time slots between adjacent operations.

instance, when an operation has a low degree of uncertainty and its execution time shows minimal fluctuations, it leads to decreased importance levels or priorities for the adjacent gap time slots. Thus, the function $h(\bullet)$ is employed to describe the impact or priorities of the random variables in the adjacent operations of a gap time slot on that specific gap time slot. The function $h(\bullet)$ can exhibit variability across different uncertain scenarios. In the scenario studied within this paper, because the operation time follows a *Normal* distribution, the function $h(\xi_{ij}, \xi_{i(j\pm1)})$ or $h\left(\xi_{ij}, \xi_{ij}\right)$ can be expressed as $\alpha \bullet \left[SD\left(\xi_{ij}\right) + SD\left(\xi_{i(j\pm1)}\right)\right]$ or $\alpha \bullet \left[SD\left(\xi_{ij}\right) + SD\left(\xi_{ij}\right)\right]$, respectively. Here, α represents a positive coefficient, and $SD(\bullet)$ denotes the standard deviation of the random variable.

(5) ***The fourth step: Calculating the dispersion degree of each dotted line (gap time slot)***.

If the $I_{G^k_{ij}}$ or $I_{G_{ij}}$ equals to 0, $-I_{G^k_{ij}} \bullet \ln I_{G^k_{ij}}$ and $-I_{G_{ij}} \bullet \ln I_{G_{ij}}$ would become undefined. To address this, intermediate variables $d_{G^k_{ij}}$ and $d_{G_{ij}}$ are introduced, as defined in Eqs. (46)-(47).

$$d_{G_{ij}} = \begin{cases} 0, if I_{G_{ij}} = 0 \\ -I_{G_{ij}} \bullet \ln I_{G_{ij}}, if I_{G_{ij}} \neq 0 \end{cases} \forall i \in C, j \in J \text{ (46)}.$$

$$d_{G^k_{ij}} = \begin{cases} 0, if I_{G^k_{ij}} = 0 \\ -I_{G^k_{ij}} \bullet \ln I_{G^k_{ij}}, if I_{G^k_{ij}} \neq 0 \end{cases} \forall i \in C, k \in K \text{ (47)}.$$

The intermediate variables are referred to as the dispersion degrees of the gap time slots. A higher importance degree does not necessarily indicate a greater dispersion degree. This approach enables the incorporation of both the importance degree and distribution of the gap time slots, resulting in a more comprehensive perspective.

(6) ***The fifth step: Calculating the structure entropy of the pre-scheduling plan network***.

$R(\boldsymbol{S}) = \sum d_{G^k_{ij}} + \sum d_{G_{ij}}$ (48).

The final step involves summing up the dispersion degrees of all gap time slots according to Eq. (48). $R(\boldsymbol{S})$ is referred to as the anti-cascade effect and robustness evaluation index of the pre-scheduling plan $\boldsymbol{S}$. The value of $R(\boldsymbol{S})$ increases as the number of gap time slots and their even distribution increase. While standard deviation can assess the distribution of gap time slots, it does not capture the quantitative information of gap time slots. Therefore, if the robustness evaluation index is constructed solely based on standard deviation, it becomes necessary to consider multiple parameters such as standard deviation, mean value, and total value comprehensively. If that is the case, the approach will indeed become more complex and cumbersome.

6. Bi-objective robust optimization model solution algorithm

6.1. Flows of solution algorithm based on NSGA-II

By applying NSGA-II, a set of Pareto frontier solutions can be obtained. Let's denote S_F as the set of feasible solutions, S_D as the set of dominated solutions, and S_P as the set of Pareto frontier solutions. We have $S_F \backslash S_P = S_D$. If S_i and S_j represent solutions, the Pareto frontier solution in this paper satisfies the following two properties: (i) $\forall S_i, S_j \in S_P$, we have $[f_1(S_i) \le f_1(S_j) and f_2(S_i) \ge f_2(S_j)] or [f_1(S_i) \ge f_1(S_j) and f_2(S_i) \le f_2(S_j)]$. (ii) $\forall S_i \in S_P, S_j \in S_D$, we have $f_1(S_i) \le f_1(S_j) and f_2(S_i) \le f_2(S_j)$. As NSGA-II is a well-established algorithm, in this paper, we only provide an overview of its fundamental procedure.

Step 1: Initialize the population of chromosomes according to the defined encoding rule.

Step 2: Perform non-dominated ranking on the chromosomes within the population and categorize them into several rankings.

Step 3: Calculate the crowding distance of chromosomes in the population, which can be used to evaluate the diversity of the population.

Step 4: Initialize the iteration counter c to 1.

Step 5: Generate the parent population by binary tournament selection.

Step 6: Generate the offspring population through crossover and mutation operations applied to the parent population, based on a specified probability.

Step 7: Merge the parent population and offspring population to form a new population.

Step 8: Perform non-dominated ranking on the chromosomes within the new population and categorize them into several rankings.

Step 9: Calculate the crowding distance of chromosomes in the new population.

Step 10: Create the new offspring population using an elite strategy.

Step 11: If $c \ge maximum\,generations$, go to Step 12, otherwise $c += 1$ and go back to Step 5.

Step 12: Output the solutions on the Pareto frontier.

Step 13: Select the most appropriate solution as the final solution for execution.

6.2. Coding, crossover, and mutation rules for chromosomes

The coding, crossover, and mutation rules for chromosomes are developed individually based on the specific problem and mathematical model. These rules play a crucial role in the implementation of the NSGA-II.

6.2.1. Coding rule

The chromosome is composed of a two-layer sequence of integer numbers. The top layer of the chromosome represents the operation tasks assignment and sequence of inbound containers, while the bottom layer represents the operation tasks assignment sequence of outbound containers. Each layer of the chromosome consists of four segments. The four segments represent the containers, QCs, IGVs and YCs, respectively.

When generating a chromosome, the sequence of container numbers in the containers segment is randomized, and the numbers representing IGVs of the upper layer are also randomized. The number representing QCs and YCs is generated according to the pre-determined assignments of QCs and YCs. Considering the double-cycling operation mode, the numbers representing IGVs in the bottom

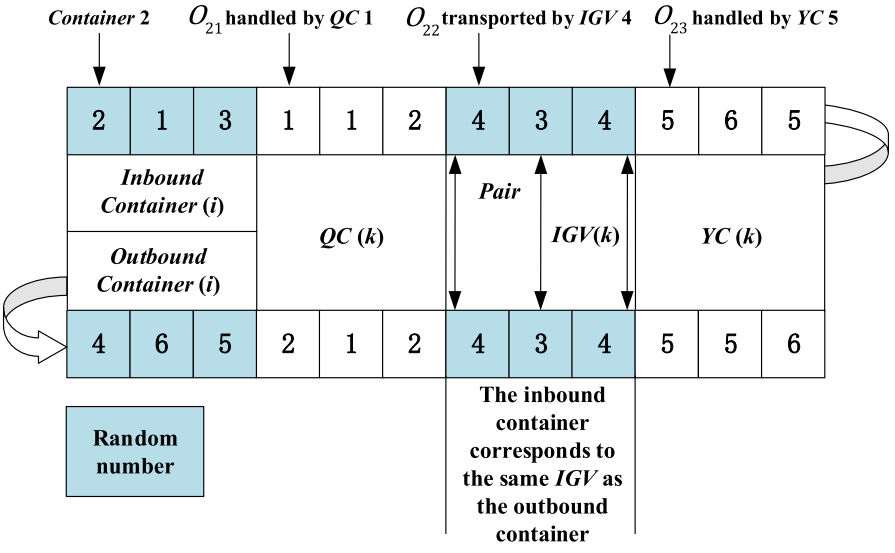

Fig. 9. A chromosome representing the scheduling of 3 inbound containers and 3 outbound containers.

layer are generated with the same values as those in the upper layer, maintaining the correspondence between the two layers.

The number in the same position of each segment has a one-to-one correspondence, indicating the assignment of tasks. Additionally, the sequential arrangement of equipment numbers from left to right is directly linked to the operation sequence of containers for each equipment. Thus, a scheduling plan chromosome is constructed to represent the integrated scheduling of multiple port equipment, taking into account the double-cycling operation mode.

An example of integrated equipment scheduling for three inbound containers and three outbound containers is illustrated in Fig. 9. Taking inbound container 2 as an example, it will be unloaded by QC 1 from the vessel onto IGV 4, transported by IGV 4 from the quay shore to the yard, and finally loaded by YC 5 from IGV 4 onto the yard. Taking IGV 3 as an example, it will transport inbound container 1 from the quay shore to the yard, and then transport outbound container 6 from the yard to the quay shore, forming a double-cycling operation.

6.2.2. Crossover rule

The crossover operation may not occur on all containers. Each container has a probability of being selected for the crossover operation. After the crossover operation, the two parent chromosomes are transformed into two offspring chromosomes. An example of the crossover operation performed on the two chromosomes is illustrated in Fig. 10. The crossover operation involves the selected inbound containers 2 and 3, as well as the outbound container 5 with the two parent chromosomes. The selected containers' numbers and their corresponding equipment's numbers are swapped between the parent chromosomes. When performing the crossover operation, the relative sequence of the numbers is preserved. This means that the order of the selected containers' numbers and their corresponding equipment's numbers remain unchanged after the exchange between the parent chromosomes. It is worth mentioning that for the crossover operation of outbound containers in Fig. 10, as there is only one outbound container requiring the crossover operation, the off-spring chromosomes related to outbound containers remain unchanged alongside the parent chromosomes. This is a potential occurrence in real crossover operations.

6.2.3. Mutation rule

The mutation operations involve the exchange of positions for inbound or outbound containers and the change of the IGV number. The occurrence probability of the mutation operation is typically low. For example, the mutation of inbound containers 2 and 3, as well as outbound containers 5 and 6, are illustrated in Fig. 11. This mutation results in an exchange of the containers' numbers and the corresponding QCs and YCs' numbers. Additionally, IGV 4 at position 9 of the chromosome undergoes a mutation and is changed to IGV 3.

6.3. Selection rule for the most appropriate solution

Let f_{1min}, f_{2min} be the minimum values of the two objectives represented in the Pareto frontier, and let IP be the ideal point with objective values equal to f_{1min}, f_{2min}. To obtain the most appropriate solution from the Pareto frontier, the Euclidean distances $ED(IP, S_i)$ between the solutions in the Pareto frontier $S_i \in \boldsymbol{S_P}$ and the IP needs to be calculated (see Fig. 12).

$$ED(IP, S_i) = \sqrt{[f_1(S_i) - f_{1min}]^2 + [f_2(S_i) - f_{2min}]^2}, \forall S_i \in \boldsymbol{S_P} \quad (49).$$

However, since the dimensions of f_1 and f_2 may be different, it may not be appropriate to calculate the Euclidean distances $ED(IP, S_i)$ directly between the solutions in the Pareto frontier $S_i \in \boldsymbol{S_P}$ and the IP. To address this issue, it is necessary to normalize the objective values of each solution and the IP, and replace the original values with their normalized values in Eq. (50). The modified equation is as follows.

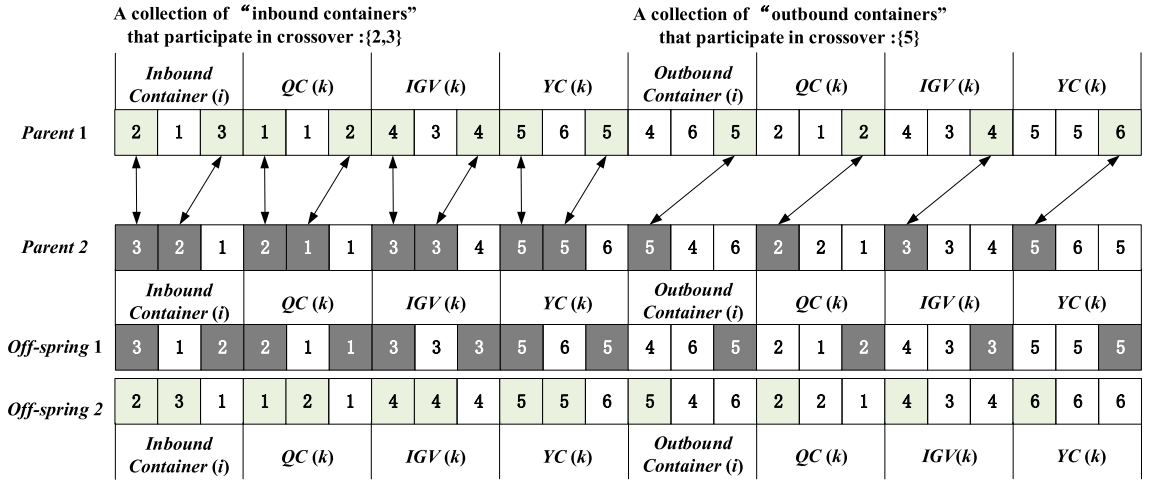

Fig. 10. The crossover operation of the two chromosomes.

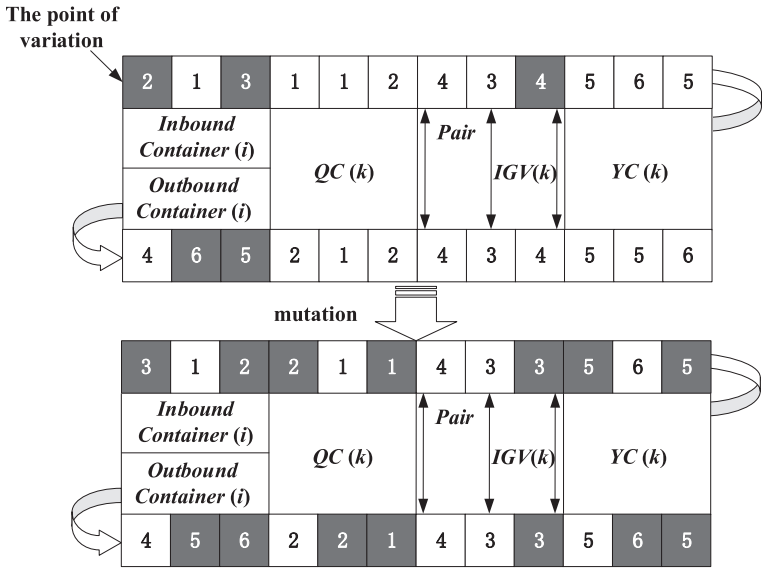

Fig. 11. The mutation operation of a chromosome.

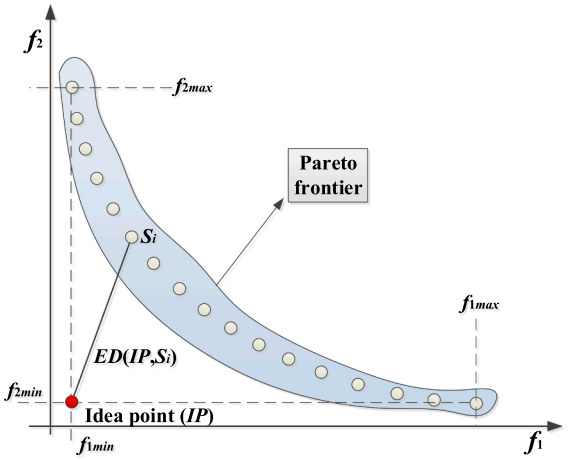

Fig. 12. Schematic representation of Euclidean distances between the idea point and the solution S_i.

$$ED'(IP,S_i) = \sqrt{\left[\frac{f_1(S_i)-f_{1min}}{f_{1max}-f_{1min}}\right]^2 + \left[\beta \bullet \frac{f_2(S_i)-f_{2min}}{f_{2max}-f_{2min}}\right]^2}, \forall S_i \in \boldsymbol{S_P} \quad (50).$$

The solution that corresponds to the minimum $ED'(IP,S_i)$ will be selected as the most suitable solution. In practical terms, when the fluctuation of the uncertain operation time is small, the value of $\beta \in [0,1]$ can also be small, indicating that the importance of the robustness of the scheduling plan is relatively low in such cases.

Table 4
Parameters settings of experimental cases.

Parameters	value	Parameters	value
The number of inbound and outbound containers handling tasks	16 ~ 2000	The maximum number of QCs	3
The maximum number of YCs	2	The maximum number of IGVs	72
Operation time of cranes	A *normal* distribution (100, σ_1^2) (s)	Movement time of cranes	A *normal* distribution (0.75, σ_2^2) (m/s)
Movement time of IGVs	A *normal* distribution (4.8, σ_3^2) (m/s)	The layout of the port	U-shaped

Table 5
Parameters settings of GA.

Parameters	value	Parameters	value
The number of chromosomes within a population	100–300	The probability of crossover operation	0.5
The probability of mutation operation	0.1	The iterative generations of chromosomes	1000–2500

7. Experiments and discussion

This section first introduces the methods that will be compared with our method. To ensure a fair comparison, all the methods share the same GA kernel. The section then presents the experimental cases and their associated parameters. Finally, the experimental results are discussed, providing insights and analysis.

7.1. Experimental settings

The task information, distances between different positions in the port, the layout of the port, and the operation time and movement speed of the equipment are obtained from real port cases. The values of the parameters are provided in Table 4.

As aforementioned, the same GA kernel is used. The number of iterative generations, the population size of chromosomes, and the probabilities of crossover and mutation are consistent across all methods in the same experimental case. The values of these parameters are shown in Table 5.

Additional parameter values can be found in Table 6. In the new method, α is the positive coefficient used in the importance of gap time slots functions, and β represents the weight of robustness in the modified Euclidean distances function. Furthermore, N_{SAA} signifies the number of sample scenarios employed in the Stochastic Programming (SP) method, as explained in Section 7.2.1. Additionally, γ represents the weight allocated to the total quantity of gap time slots in the Maximum Gap (MG) method, as detailed in Section 7.2.4.

All experiments were conducted on a PC with a 64-bit Windows 10 system, running on an Intel i9-11900 processor with a clock speed of 2.50 GHz and 32 GB of memory. The programs were executed using MATLAB R2022a.

7.2. Comparative methods

This paper compares the performance of four commonly used methods belonging to the proactive scheduling approaches: SP, Robust Optimization (RO), Triangle Fuzzy Programming (TFP), and MG methods (see Table 7). These methods are compared with our newly proposed method to evaluate the effectiveness and performance of our method. In the comparison analysis, all the methods, including our new method, SP, RO, TFP, and MG, are based on the same GA kernel. This means they share key elements, from chromosome encoding and decoding rules to chromosome crossover and mutation rules. Additionally, they use the same probabilities for crossover and mutation events, and maintain consistent numbers of iterative generations and population sizes under the same experimental case. The reasons for not using solvers like CPLEX and Gurobi to solve the model include: 1) The mixed-integer programming model discussed in this paper encompasses numerous variables and constraints, in addition to uncertain parameters. Therefore, it becomes overly time-consuming and impractical to use a solver to solve the model. 2) While solvers are capable of addressing comparative methods like SP and RO, the proposed method in this study, which constitutes a bi-objective optimization model extending beyond the classical SP and RO, cannot be directly tackled through solver-based approaches. Consequently, a heuristic approach is employed to solve the proposed mixed-integer programming model.

7.2.1. Stochastic programming method

The SP method has been widely applied to solve various port equipment scheduling problems, such as QCSP (Ma et al., 2021), YCSP (Zheng et al., 2019), BACASP (Han et al., 2010), and IVSP (Li et al., 2023b), concerning uncertain operation time. Similar to the approach taken by the above studies, in the SP method used for comparison in this paper, the expectations of functions related to uncertain parameters have been optimized. In the SP method, the objective function (1) is reformulated as follows:

$$Minimize\ f = \mathbb{E}(makespan) = \mathbb{E}(C_{max}) \quad (51).$$

where the term "$\mathbb{E}(makespan)$" signifies the expected value of *makespans* under all uncertain scenarios.

An approach known as Sample Average Approximation (SAA) is adopted to handle the matter of expectation value of the objective function. The fundamental idea behind SAA is to generate a collection of samples through the extraction of uncertain parameter values from probability distributions representing uncertainty integrated with a Monte Carlo Simulation (MCS) method. With a sufficiently large sample size, the average value of the objective function derived from these samples closely approximates the real expectation

Table 6
Other parameters settings.

Parameters	value	Parameters	value
α	2	β	0.01
N_{SAA}	10	γ	0.01

Table 7
Attributes of the comparative methods and the new method.

Methods	Advantages	Fitness	Limitations	References
SP	Solid theoretical foundation	The probability distribution of uncertainty is needed	Much prior knowledge is needed, and it is often difficult to obtain in reality; Too much computation time	Han et al., 2010; Li et al., 2023b; Liu et al., 2022; Ma et al., 2021; Zheng et al., 2019
RO	Excellence in the worst-case	The value range of uncertainty is needed	Too conservative	Rodrigues and Agra, 2021
TFP	Easy to operate and flexible	The triangle fuzzy numbers of uncertainty are needed	Much computation	Expósito-Izquiero et al., 2016
MG	Easy to operate; Less computation time	A small amount of information about uncertainty or even no information is needed	Poor effectiveness	Dik and Kozan, 2017; Yu et al., 2021
The new method	Good effectiveness when facing a large degree of uncertainty; Less computation time	A small amount of information about uncertainty or even no information is needed	High requirement for learning and need of time for its popularity	This paper

Table 8
Average *makespans* of 20,000 simulation experiments and CPU times.

Case size	Uncertainty degree	SP		RO		TFP		MG		Our method	
		Makespan (s)	CPU (s)	*Makespan* (s)	CPU (s)	*Makespan* (s)	CPU (s)	*Makespan* (s)	CPU (s)	*Makespan* (s)	CPU (s)
8/8/1/3/2	5–0.04–0.3	4697.51 ± 0.63	905.84	4697.67 ± 0.63	**50.67***	4697.61 ± 0.63	190.1	4697.65 ± 0.63	54.80	4697.17 ± 0.63	96.89
	10–0.08–0.6	4717.10 ± 1.27	923.34	4714.73 ± 1.28	**49.67***	4717.17 ± 1.26	184.95	4716.23 ± 1.27	51.13	4716.59 ± 1.28	106.31
	15–0.12–0.9	4752.13 ± 1.97	897.83	4751.52 ± 1.99	**48.84***	4750.86 ± 2.00	184.05	4751.46 ± 2.00	48.91	4750.91 ± 1.99	100.69
	20–0.15–1.2	4819.91 ± 6.64	878.30	4812.80 ± 5.20	**49.31***	4817.25 ± 3.27	185.52	4829.35 ± **26.9** Δ	54.84	4815.46 ± 3.39	107.05
15/15/2/5/2	5–0.04–0.3	4634.36 ± 0.59	1677.98	4551.83 ± 0.60	**123.61***	4497.13 ± 0.59	303.03	4486.91 ± 0.59	130.61	**4478.80 ± 0.59***	128.30
	10–0.08–0.6	4606.83 ± 1.23	1687.17	4691.80 ± 1.25	**123.66***	4543.09 ± 1.20	304.03	4595.75 ± 1.22	128.47	**4532.00 ± 1.17***	126.11
	15–0.12–0.9	4581.62 ± 1.98	1690.06	4656.71 ± 1.91	**123.56***	4719.14 ± 1.95	307.05	4700.57 ± 1.89	126.34	4577.98 ± 1.97	126.91
	20–0.15–1.2	4716.87 ± 5.98	1357.69	4701.77 ± 8.20	122.33	4685.69 ± 3.40	306.72	4783.99 ± 5.51	126.25	**4672.03 ± 6.37***	**119.72***
30/30/2/7/2	5–0.04–0.3	**8791.94 ± 0.83***	3183.03	8855.42 ± 0.83	327.02	8968.21 ± 0.82	737.66	8805.84 ± 0.79	**299.19***	8801.07 ± 0.80	392.86
	10–0.08–0.6	8957.76 ± 1.68	3228.72	9182.79 ± 1.71	337.17	**8932.97 ± 1.67***	850.69	8949.70 ± 1.62	**336.50***	8996.11 ± 1.67	498.20
	15–0.12–0.9	8968.62 ± 2.54	3276.55	8932.52 ± 2.55	**258.00***	8954.66 ± 2.55	816.95	8939.79 ± 2.51	345.25	**8897.60 ± 2.51***	511.47
	20–0.15–1.2	9155.65 ± 9.86	3224.25	9115.64 ± 10.2	**292.73***	9190.07 ± 12.0	836.95	9209.85 ± **32.3** Δ	320.97	**9046.49 ± 7.90***	623.13
60/60/2/20/2	5–0.04–0.3	16945.8 ± 1.14	15773.8	16731.9 ± 1.14	1636.45	16739.4 ± 1.11	4698.17	16894.6 ± 1.14	**1540.97***	**16728.4 ± 1.14***	2282.72
	10–0.08–0.6	**16664.0 ± 2.22***	15771.6	17194.1 ± 2.28	1635.42	17194.6 ± 2.26	4766.44	17191.7 ± 2.25	**1572.83***	16751.6 ± 2.21	2873.42
	15–0.12–0.9	17039.3 ± 3.53	15889.5	16941.7 ± 3.54	1614.78	**16659.5 ± 3.48***	4677.83	17250.5 ± 3.46	**1299.30***	16957.2 ± 3.36	1529.63
	20–0.15–1.2	17133.0 ± **480** Δ	15776.1	17375.1 ± 24.1	1631.16	17158.4 ± 15.9	4703.41	17582.7 ± 18.6	**1570.25***	17088.0 ± 22.4	2267.11
100/100/2/35/2	5–0.04–0.3	27935.7 ± 1.44	53350.5	28509.7 ± 1.50	3554.44	27794.6 ± 1.46	11429.22	28160.5 ± 1.46	**3483.91***	**27722.4 ± 1.44***	4823.00
	10–0.08–0.6	27794.8 ± 2.87	51685.0	28616.5 ± 3.00	**3118.06***	**27561.7 ± 2.90***	8714.61	29089.3 ± 2.96	3512.86	27593.3 ± 2.89	4078.47
	15–0.12–0.9	28102.3 ± 4.54	52926.1	**27636.0 ± 4.48***	4032.64	27952.6 ± 4.45	9759.50	29368.0 ± 4.61	**2995.41***	28941.2 ± 4.61	4386.67
	20–0.15–1.2	29035.6 ± **119** Δ	53580.8	29167.2 ± 36.6	**3840.77***	29888.9 ± **1176** Δ	7110.53	29177.6 ± **409** Δ	4209.83	**28015.4 ± 28.1***	6437.53
250/250/3/45/2	5–0.04–0.3	51855.5 ± 1.98	129,090	50701.8 ± 2.14	**9813.58***	50683.2 ± 1.96	24225.2	52104.3 ± 2.00	11718.8	**49222.6 ± 1.87***	10926.0
	10–0.08–0.6	50194.6 ± 3.85	127,827	51083.8 ± 4.01	**9792.58***	51251.3 ± 3.96	24006.1	52202.8 ± 3.93	11670.4	**49198.0 ± 3.68***	10943.9
	15–0.12–0.9	51795.7 ± 6.06	127,765	53821.7 ± 8.59	**9535.02***	52205.9 ± 6.11	23312.4	53350.3 ± 6.20	11228.9	**50188.0 ± 5.77***	11187.0
	20–0.15–1.2	53758.7 ± 53.15	128,169	55971.7 ± **289** Δ	**9746.56***	53162.0 ± 62.4	24153.7	53144.4 ± 82.5	11196.7	**50614.4 ± 65.8***	11356.9
500/500/3/56/2	5–0.04–0.3	111,797 ± 3.00	348,220	110,348 ± 2.96	**27645.1***	112,580 ± 2.97	71803.4	114,470 ± 2.98	27869.5	**110,112 ± 2.93***	34513.5
	10–0.08–0.6	113,597 ± 5.96	360,442	112,238 ± 5.98	**27490.3***	111,858 ± 5.96	80398.8	115,397 ± 6.11	27672.4	**108,558 ± 5.81***	31296.3
	15–0.12–0.9	111,973 ± 9.10	352,051	117,846 ± 9.34	**27616.2***	113,066 ± 9.15	80798.6	116,425 ± 9.29	27712.6	**107,408 ± 8.66***	33370.3
	20–0.15–1.2	116,104 ± 44.2	358,198	119,581 ± **649** Δ	**27413.2***	116,160 ± **128** Δ	79660.1	119,184 ± **570** Δ	27658.4	**114,271 ± 95***	33483.2
1000/1000/3/72/2	5–0.04–0.3	**244,447 ± 4.44***	727,836	246,242 ± 4.42	64688.2	247,434 ± 4.46	157875.6	248,997 ± 4.50	56952.8	245,662 ± 4.47	**50749.8***
	10–0.08–0.6	244,749 ± 8.87	748,056	251,379 ± 9.11	70409.6	246,896 ± 9.01	153,290	254,849 ± 9.09	69749.2	**243,476 ± 8.52***	**47309.1***
	15–0.12–0.9	250,398 ± 13.9	757,026	252,951 ± 14.0	70007.4	254,051 ± 13.8	153,549	252,903 ± 14.2	70295.7	**241,306 ± 13.5***	**50592.3***
	20–0.15–1.2	258,009 ± 202	737,705	263,082 ± 362	70180.3	256,318 ± 368	153,203	257,941 ± 374	70068.9	**250,527 ± 189***	**50538.6***
Winning count		3	0	1	**19***	3	0	0	8	**19***	5

Notes:
Case size indicates No. of inbound containers/No. of outbound containers/No. of QCs/No. of IGVs/No. of YCs.
Uncertainty degree indicates standard deviation of operation time and movement speed ($\sigma_1^2 - \sigma_2^2 - \sigma_3^2$).
"±" indicates 99% confidence intervals for the *makespans*.
"*" indicates the best result within a scenario of a case.
"Δ" indicates the *makespans* of the scheduling plan exhibit significant fluctuations compared to others within a specific case scenario, primarily attributable to the influence of uncertainty and its consequent cascading effects. This observation also suggests that the scheduling plan possesses comparatively limited anti-cascade effects and robustness.

value of the objection function in SP, in accordance with the law of large numbers. The employment of SAA has garnered recognition in recent years for its application in resolving port resource scheduling problems that embrace uncertainty in the realm of SP (Li et al., 2023b; Zheng et al., 2019).

Nonetheless, while an increased quantity of samples tends to enhance the quality of solutions in SAA, it simultaneously engenders a significant rise in computation time (Han et al., 2010; Li et al., 2023b; Zheng et al., 2019). In this study, 10 sample scenarios within the framework of SAA are employed to circumvent the extensive computation time.

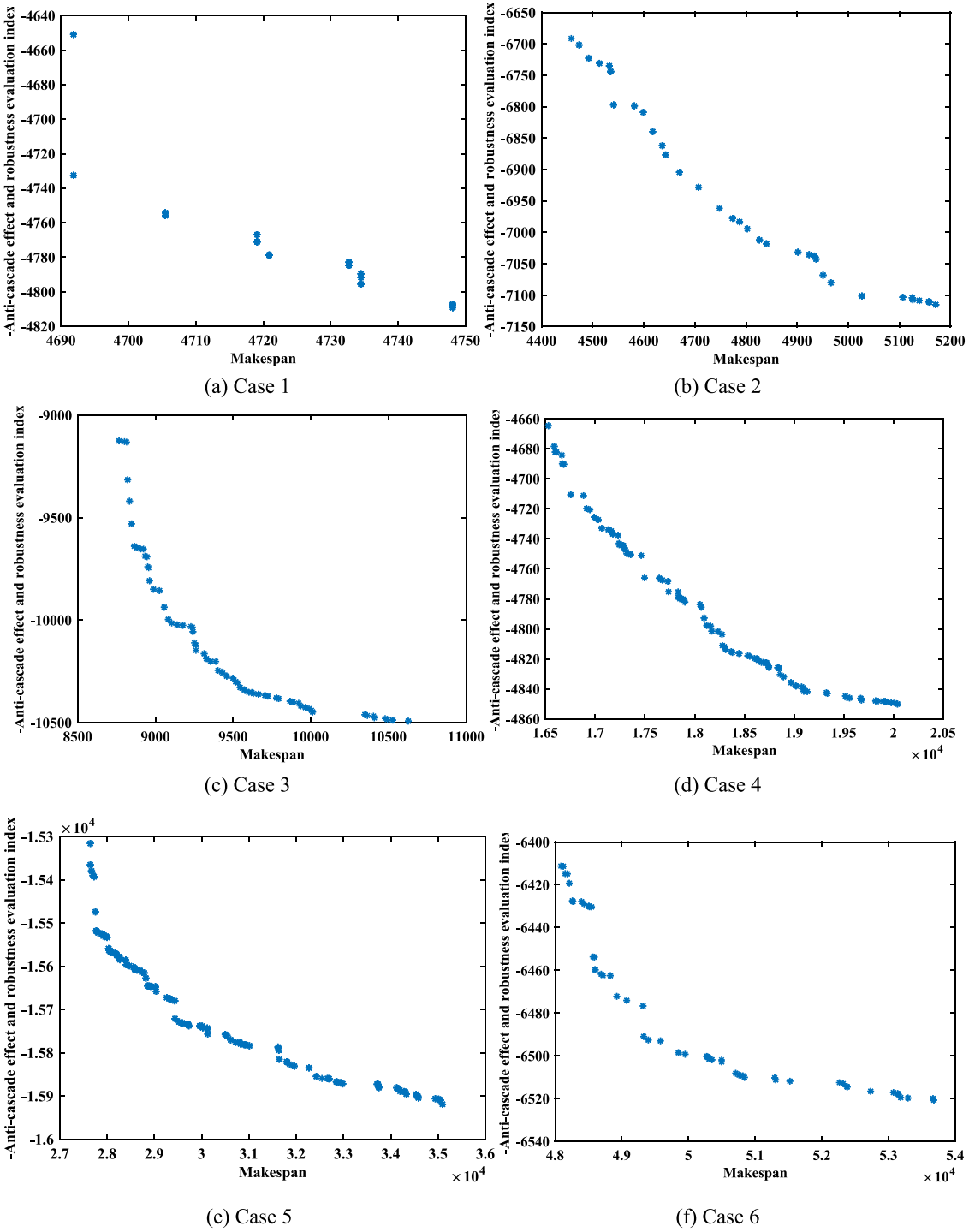

Fig. 13. Pareto frontiers of the new method.

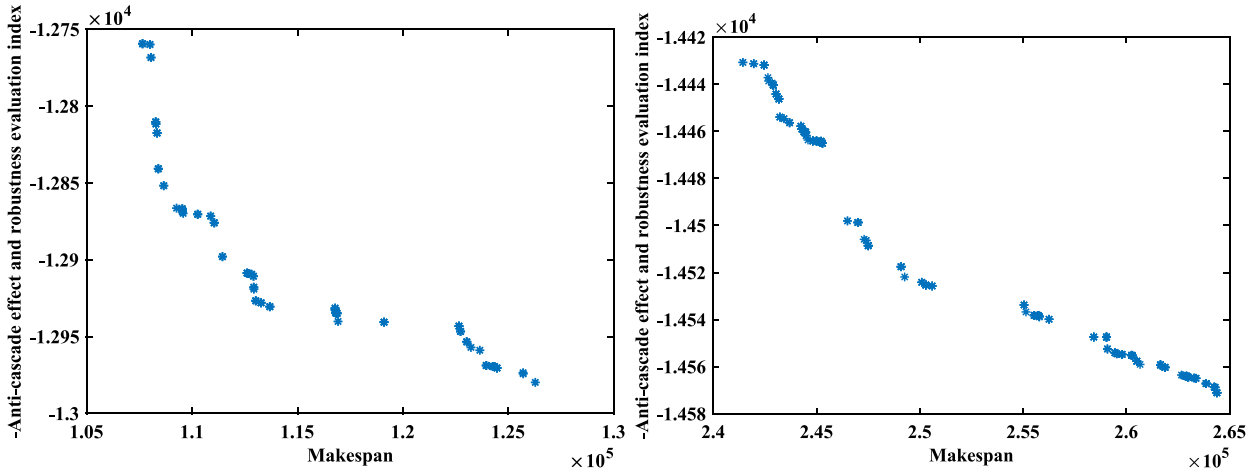

Fig. 13. (*continued*).

7.2.2. Robust optimization method

The RO method is utilized to address uncertain problems where the probability distribution of uncertain parameters is unknown, but the value range or uncertainty set is known. In RO, the objective is to optimize the worst-case scenario to ensure that the pre-scheduling plan remains feasible for all scenarios related to uncertainty. In the RO method, the objective function (1) is reformulated as follows:

$$Minimize\, f = \max_{\tilde{t}_{ij}\in T_{ij},\tilde{v}_k\in V_{ij},\forall i\in C,j\in J} makespan = \max_{\tilde{t}_{ij}\in T_{ij},\tilde{v}_k\in V_{ij},\forall i\in C,j\in J} C_{max} \quad (52).$$

where $\tilde{t}_{ij}$ and $\tilde{v}_k$ represent uncertain parameters, as previously detailed, and T_{ij} and V_{ij} denote the value sets for these uncertain parameters. The expression $\max_{\tilde{t}_{ij}\in T_{ij},\tilde{v}_k\in V_{ij},\forall i\in C,j\in J} makespan$ pertains to the worst-case scenario arising from such uncertainties. Consequently, the primary goal of this objective is to optimize the outcome under the most unfavorable circumstances precipitated by these uncertainties.

The RO method has been employed to solve the BACASP while concerning uncertain vessel arrival times, as demonstrated by Rodrigues and Agra (2021). In the RO method used for comparison in this paper, the maximum values of the uncertain parameters are utilized to represent the worst-case scenarios.

7.2.3. Triangle fuzzy programming method

In the TFP method, uncertain parameters are represented using triangular fuzzy numbers (Lei, 2012). Expósito-Izquiero et al. (2016) applied this method to solve BACASP. They defined fuzzy membership functions for uncertain arrival times of vessels and uncertain processing times of operations. Similarly, in TFP used for comparison in this paper, associated fuzzy membership functions, as well as operation and comparison rules, are defined for triangular fuzzy numbers. If $\tilde{b}$ represents the uncertain parameter, it can be further defined as $\tilde{b} = (b_{\min}, b, b_{\max})$ in our paper, where the $b_{\min}$,b and $b_{\max}$ are the minimum, average and maximum values of the uncertain parameter, respectively. Let $\tilde{b}'$ represent another uncertain parameter. The sum and difference operations of triangle fuzzy number are defined as follows:

$$\tilde{b} \pm \tilde{b}' = (b_{\min} \pm b'_{min}, b \pm b', b_{\max} \pm b'_{max}) \quad (53).$$

The $\mu\left(\tilde{b}\right)$ is used to compare fuzzy numbers, and $\tilde{b} \le \tilde{b}'$ when $\mu\left(\tilde{b}\right) \le \mu\left(\tilde{b}'\right)$. $\mu\left(\tilde{b}\right)$ is defined as follows:

$$\mu\left(\tilde{b}\right) = (b_{\min} + 2b + b_{\max})/4 \quad (54).$$

7.2.4. Maximum gap method

In the MG method, the schedules with the largest sum of gap time slots are selected. The gap time slots are considered as buffers that can absorb some uncertainty. This method has been applied to solve the QCSP concerning uncertain handling times of QCs (Dik and Kozan, 2017), and the BACASP concerning uncertain arrival times of vessels (Yu et al., 2021). In the practical application of this study, the objective function (1) is reformulated as follows:

$$Minimize\, f = min\left[makespan - \gamma \bullet \left(\sum G_{ij}^k + \sum G_{ij}\right)\right] \quad (55).$$

where $(\sum G_{ij}^k + \sum G_{ij})$ represents the total gap time slots of a pre-scheduling plan, and γ means the weight assigned to $(\sum G_{ij}^k + \sum G_{ij})$. While the quantity of gap time slots has received attention from some researchers, the distribution of these gaps has not been sufficiently paid attention to. This paper fills this research gap.

7.3. Results of the experiments

The experiments were carried out on various scales of cases, each with a different number of inbound containers, outbound containers, and equipment. Each case was assigned four degrees of uncertainty, which were measured by the standard deviation of the

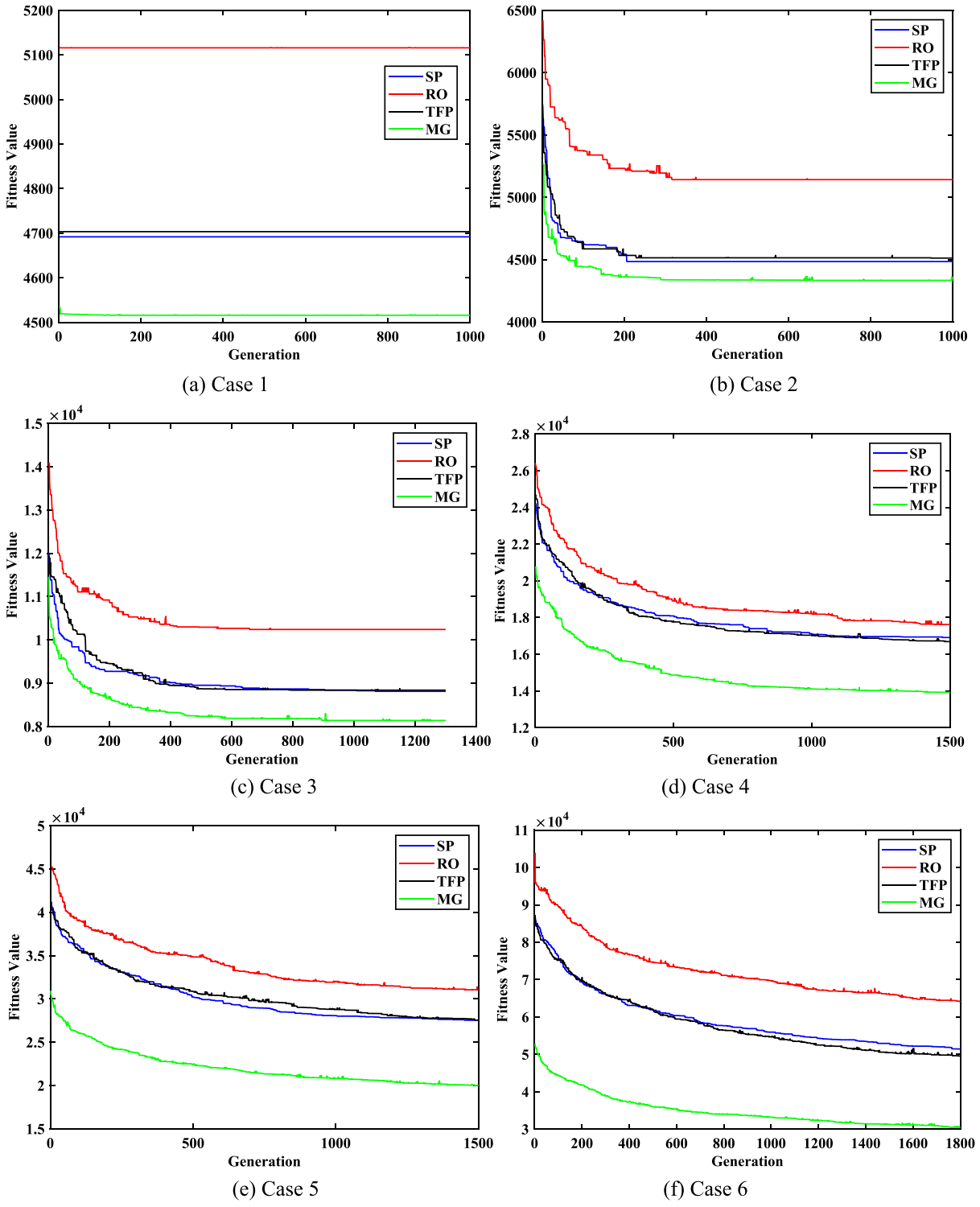

Fig. 14. Convergence curves of compared methods.

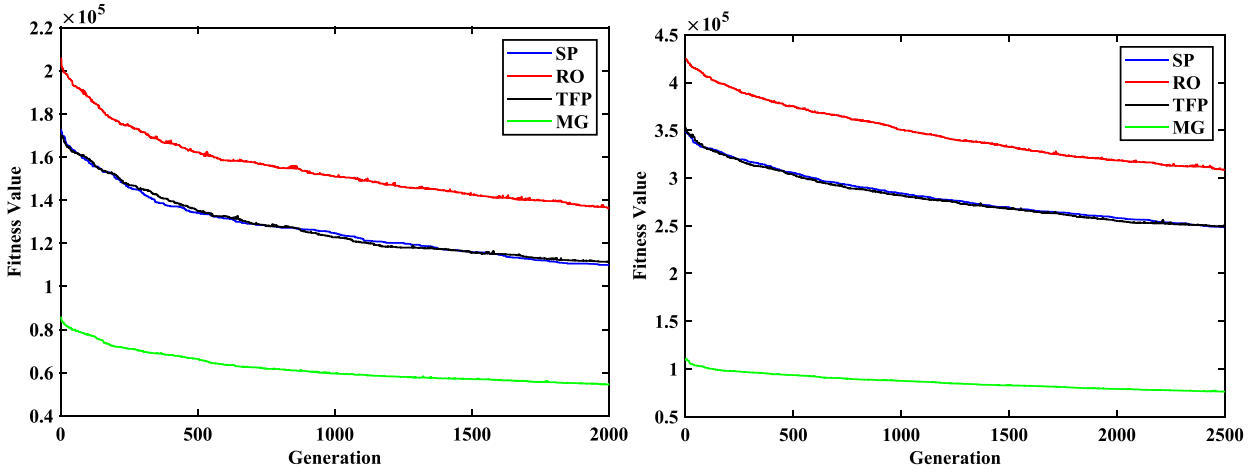

Fig. 14. (*continued*).

uncertain parameters. A higher standard deviation indicated a higher degree of uncertainty.

To evaluate the performance of the different methods, the pre-scheduling plans generated by each method were implemented in a simulation environment that incorporated uncertainty. Each experiment was repeated 20,000 times, and the average *makespans* of these repeated experiments were recorded. Additionally, the CPU times required for generating the pre-scheduling plans were also recorded.

Table 8 presents the performance results of different methods across various cases, including the average *makespans*, which indicate the execution performance of pre-scheduling plans generated by different methods, and the CPU times required for generating these pre-scheduling plans.

Based on the experimental results in Table 8, several findings are observed. Regarding the average *makespan* with 99 % confidence intervals: 1) The new method consistently outperforms the compared methods, achieving a total of 19 wins in terms of the average *makespan*. Its superiority generally becomes more pronounced as the problem scale and degree of uncertainty increase. 2) The SP, RO and TFP methods perform moderately well, winning 3, 1, and 3 counts, respectively. 3) The MG method has the worst performance with zero wins.

Regarding CPU time: 1) The new method consumes the third highest amount of computational resources but achieves the best results in terms of average *makespans*. Its CPU time is approximately 20–50 % higher than that of the RO methods, which show the lowest CPU time. However, as the problem scale expands, the excess ratio starts decreasing. It is worth noting that in the largest-scale case, the computational time of the new method is the shortest among all the methods. 2) The SP method consumes the most computation resources, which is 10–15 times greater in comparison to other methods. However, its substantial computational expenses did not yield significant improvements in *makespans* optimization. 3) The TFP method consumes the second-most computational resources, approximately 1.5 to 3 times more than the RO and MG methods, even though its performance in terms of average *makespans* is comparable to the other methods. 4) The MG method consumes slightly more computational resources than the RO method, but it performs the worst in terms of *makespan*.

Regarding 99 % confidence intervals for the *makespans*: 1) The stability of our method is exceptional as it possesses no cases in which the *makespans* of the scheduling plan exhibit significant fluctuations compared to the other concerned methods within the specific scenario containing uncertainty. 2) When the confidence intervals are introduced, various methods exhibit nearly indistinguishable performance in very small-scale cases.

The Pareto frontiers generated by the proposed method are depicted in Fig. 13. Each case consists of four scenarios with varying degrees of uncertainty. Therefore, there are a total of 32 Pareto frontier figures. However, the Pareto frontier figures within the same case exhibit minimal differences. Due to space constraints, only 8 Pareto frontier figures are shown, with each figure representing a case. In the small-scale case, the number of solutions in the Pareto frontier is limited. However, in the medium and large-scale cases, the Pareto frontier exhibits a larger number of solutions that are uniformly distributed. This demonstrates the effectiveness and efficiency of using NSGA-II in our study.

The convergence curves of the compared methods are shown in Fig. 14. Similar to Fig. 13, there are a total of 32 figures representing 8 cases and 32 scenarios. However, due to minimal differences in the convergence curves generated by the same method within the same case and space limitations, only 8 figures from 8 cases are displayed. Each figure represents a unique case. In the small-scale case, the solution algorithm converges quickly. However, in the medium-scale case, the convergence curves flatten out after numerous generations. In the large-scale case, the convergence curves exhibit a gradual and steady decline. It appears that if the iteration were to continue, the convergence curve would continue to decline further. However, due to the limitations of computation time, this could be further investigated in the future. Since the SP and TFP methods share the same fitness value function, their convergence curves can be

compared.

7.4. Discussions

The SP method performs moderately, likely because of a relatively limited number of samples utilized in SAA for computing the expectation values of the objective. Nevertheless, such a modest quantity of samples has the potential to result in impractical levels of computational time, let alone with a larger number of samples. Consequently, excessive computational time renders the SP impractical for implementation.

The RO method's solutions, which have the worst fitness values among the SP and TFP methods, align with theoretical expectations. The RO method is designed to optimize performance in the worst-case scenario, but it only outperforms in a very limited case. In most cases, its poor fitness values result in high *makespans*, rendering its conservative nature meaningless.

The TFP method, which has gained popularity in recent years, performs slightly better than the RO and SP methods. However, its relatively long computation time also poses difficulties for practical implementation. One of the challenges with the TFP method is to accurately estimate the triangle fuzzy number of uncertain operation times.

The poor experimental results of the MG method demonstrate that solely pursuing the maximum number of gap time slots is error-prone. Some large gap time slots may have minimal impact on absorbing fluctuations of uncertain operation times.

In small-scale cases, the new method demonstrates its strengths in many cases, despite showing relatively weaker performance in a limited number of alternative solutions. Indeed, in larger scale cases, where the scale of the case exceeds 100/100/2/35/2, the new method's advantages become more apparent. It aids to achieve the aim of selecting solutions that not only have better theoretical *makespans* but also possess a greater quantity of gap time slots with a more uniform distribution.

For a more in-depth analysis, Gantt charts depicting the pre-scheduling plans generated by different methods in a 30/30/3/7/3 case are presented in Fig. 15.

When examining the Gantt Charts, it can be observed that the port operations exhibit a double-cycling characteristic. After an IGV completes the operation of an inbound container from the shoreline to the yard, it immediately proceeds to transport an outbound container from the yard to the shoreline. There are interaction time slots between IGVs and cranes, which refer to the time spent by IGVs near the unloading/loading points while waiting for the crane to lower the rope. Therefore, the Gantt Charts provide evidence that the developed integrated scheduling model and related algorithm by this study greatly align with the reality and practicality of

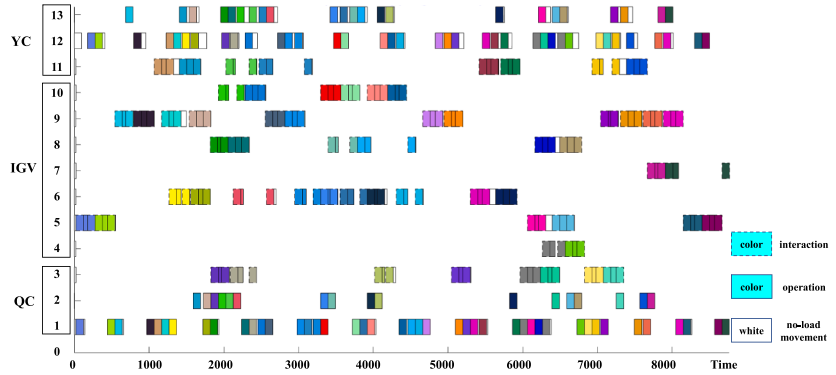

(a) The pre-scheduling plan generated by SP

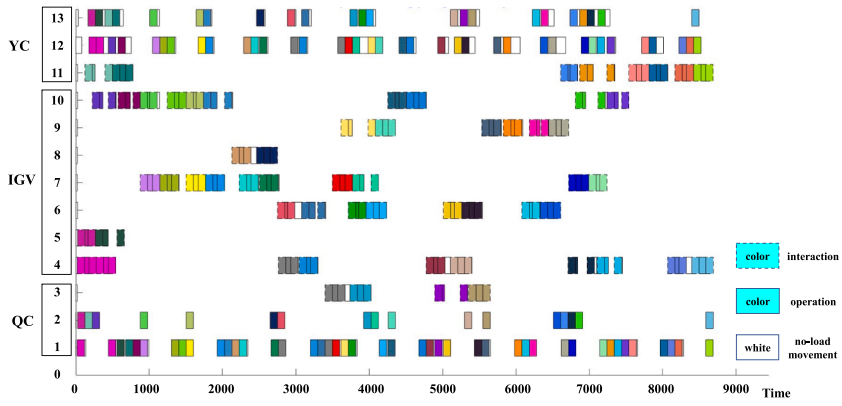

(b) The pre-scheduling plan generated by RO

Fig. 15. Gantt Charts of schedules generated by compared methods and our method in Case 3.

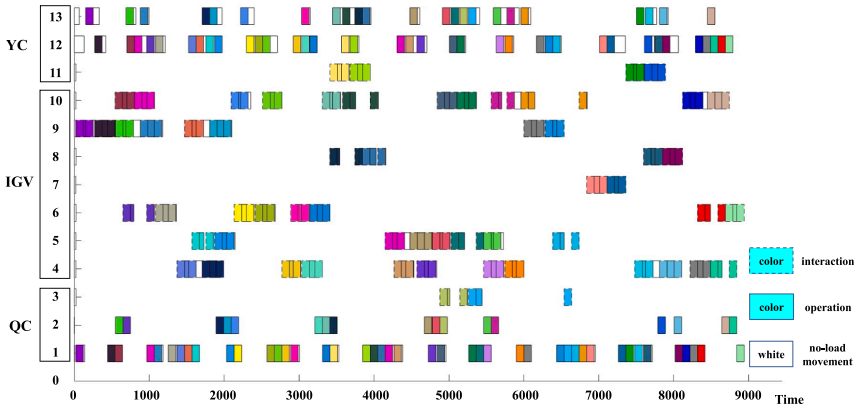

(c) The pre-scheduling plan generated by TFP

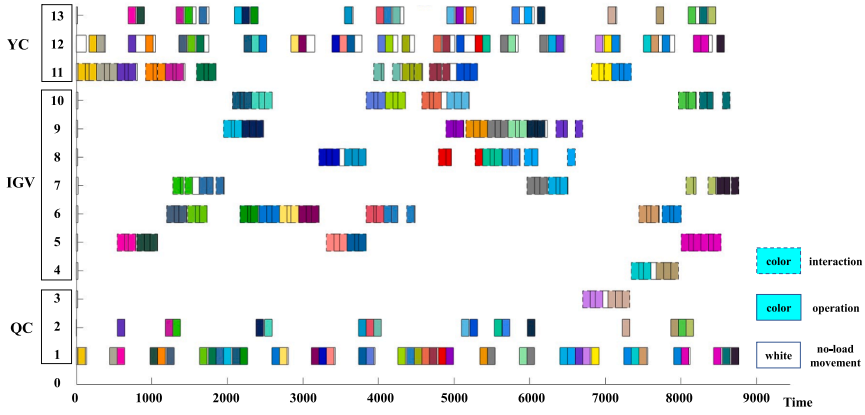

(d) The pre-scheduling plan generated by MG

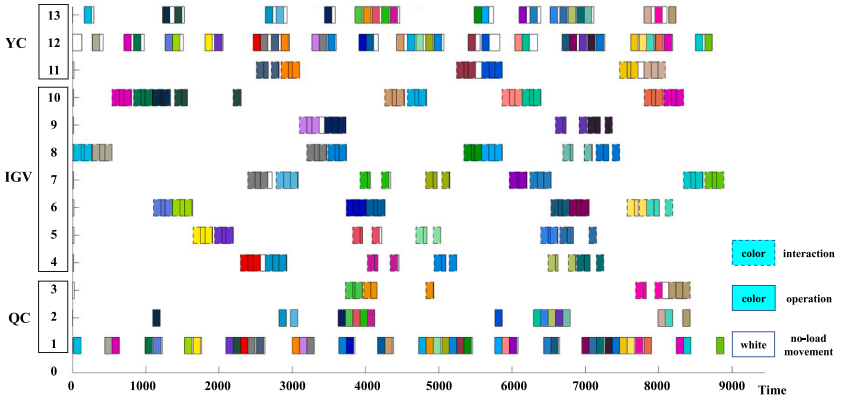

(e) The pre-scheduling plan generated by the new method

Fig. 15. (*continued*).

port operations.

All the Gantt Charts generated by different methods exhibit similar *makespans* since they share the same GA kernel with identical parameters. The RO method may have a slightly larger *makespan*, but it aligns with theoretical expectations. When considering the gap time slots, it is found that the pre-scheduling plans generated by the SP, RO, TFP, MG, and the new method have 101, 99, 97, 96, and 110 gap time slots, respectively. The schedule generated by the new method has the highest number of gap time slots. Although the MG and new methods have both revealed a high total length of gap time slots, these gap time slots in the new method are more uniformly distributed than those in the MG method. Such a substantial number of uniformly distributed gap time slots can withstand fluctuations in uncertain operation times and have therefore shown superior performance as the problem scale increases. This explains why the new method exhibits superior stability compared to others when subjected to the 99 % confidence interval test within the context of 20,000

repeated experiments conducted in an uncertain environment.

Considering the number, sum, average value, and standard deviations of gap time slots comprehensively may yield similar effects. However, this approach would involve a larger number of parameters and variables, making it more complex and challenging compared to the proposed method in this paper.

7.5. Implications

In the large-scale cases involving 2000 containers, the computation time required for the new method is approximately 14 h. Although this may seem lengthy, it does not necessarily imply impracticality, as the experiments were conducted using a personal computer. Ports typically have more powerful servers that can compute 10–20 times faster. In practical port applications, it is therefore reasonable to expect a much shorter computation time to an acceptable level. Additionally, the pre-scheduling plan is not a real-time schedule and can be created a few days in advance based on the cargo information provided by the shipping companies (Li et al., 2023a; Li and Yang, 2023). Therefore, the actual port operations may not require the pre-scheduling plan for all tasks, which require extensive computation. Instead, the port can create schedules for a subset of tasks using a rolling time window approach. From this perspective, the new method has exposed a huge potential for its applications in actual port operations.

Furthermore, the new method demonstrates strong generalization capabilities. Unlike the SP and TFP methods that require knowledge of the probability distribution or more detailed information about uncertain parameters, it does not rely heavily on precise value rules of uncertain parameters. Although having knowledge of the distribution of random variables is advantageous when calculating the importance degree of each gap time slot, even when only the average values of uncertain parameters are used, it can still be effective. In contrast, the SP, RO, and TNP methods may not be applicable in such situations.

Besides, within the RPS framework, the NSGA-II algorithm, which is a bi-objective optimization algorithm, can be replaced with other more suitable algorithms, depending on the applied context. The solution algorithm can be more adaptive to make the proposed RPS framework more generic. In this paper, the widely used and effective NSGA-II algorithm is employed for a fair comparison.

In addition to addressing integrated scheduling problems in port logistics, the new method also has the potential to be applied to solve berth allocation problems concerning the uncertain arrival time of vessels and operation time. Furthermore, it can also be applied to solve problems of workshop scheduling, warehouse sorting AGV scheduling or vehicle scheduling that consider uncertain operation times in the fields of production logistics, warehouse logistics or city logistics. The new method may have a particularly significant impact on workshop or warehouse sorting AGV scheduling scenarios. Time control is more crucial in production and sorting compared to port operations because saving time in workshops and warehouses can yield more substantial benefits. Furthermore, workshops often involve jobs with multiple operation procedures, whereas port operations typically involve three operation procedures for containers. In scenarios with large-scale and complex operation procedures, the new method exhibits a distinct advantage, making it well-suited for such applications.

8. Conclusion

More efficient operations can improve the service level of the port and reduce costs, including energy consumption. In response to this demand, a new and efficient U-shaped layout and double-cycling operation mode have emerged, placing higher requirements on the new integrated scheduling of equipment in ports. Additionally, the pervasive uncertainty and its cascade effects further complicate the formulation of pre-scheduling plans. To address these challenges, this paper proposes a proactive scheduling framework that incorporates anti-cascade effects and a robustness evolution index based on complex network entropy. The framework aids to solve the U-shaped port integrated scheduling problem involving QCs, IGVs, and YCs, while concerning uncertain operation times and the double-cycling operation mode. The experimental cases are based on real port operations, providing evidence of the practicality of the new method.

In this study, the new method is compared with four widely used and state-of-the-art proactive scheduling methods to demonstrate its superiority. The results demonstrate that it is capable of generating a robust pre-scheduling plan with a reduced *makespan*, along with a higher number of gap time slots between operations and a more uniform distribution of these gap time slots. Moreover, some implications are provided based on the findings.

One limitation of this study is that it only compares the fundamental state-of-the-art SP, RO and TFP methods. It will be insightful to take into account their extended or the combination of the new method with the SP, RO, and TFP methods. The other possible development following this research is to incorporate more relevant objectives, such as energy consumption, to improve the ability of the new method to better address the real demands. The multi-objective optimization algorithm in the new RPS framework can be further developed to achieve even higher performance.

CRediT authorship contribution statement

Lei Cai: Conceptualization, Data curation, Formal analysis, Investigation, Methodology, Resources, Software, Validation, Writing – original draft, Writing – review & editing. **Wenfeng Li:** Funding acquisition, Investigation, Methodology, Project administration, Resources, Supervision, Writing – review & editing. **Bo Zhou:** Investigation, Methodology, Supervision, Writing – review & editing. **Huanhuan Li:** Formal analysis, Investigation, Methodology, Supervision, Writing – review & editing. **Zaili Yang:** Funding acquisition, Investigation, Methodology, Project administration, Resources, Supervision, Writing – review & editing.

Declaration of Competing Interest

The authors declare that they have no known competing financial interests or personal relationships that could have appeared to influence the work reported in this paper.

Data availability

Data will be made available on request.

Acknowledgements

This research was supported by the National Natural Science Foundation of China (62173263) and China Scholarship Council (202206950005).

References

Ahmed, E., El-Abbasy, M.S., Zayed, T., Alfalah, G., Alkass, S., 2021. Synchronized scheduling model for container terminals using simulated double-cycling strategy. Computers & Industrial Engineering 154, 107118. https://doi.org/10.1016/j.cie.2021.107118.

Cahyono, R.T., Kenaka, S.P., Jayawardhana, B., . Simultaneous Allocation and Scheduling of Quay Cranes, Yard Cranes, and Trucks in Dynamical Integrated Container Terminal Operations. IEEE Transactions on Intelligent Transportation Systems 23, 8564–8578. https://doi.org/10.1109/TITS.2021.3083598.

Cai, L., Li, W., Luo, Y., 2022. Framework and Algorithm of Customized Workshop Production-logistics Collaborative Scheduling. Journal of Mechanical Engineering 58, 214–226. https://doi.org/10.3901/JME.2022.07.214.

Cai, L., Guo, W., He, L., Li, W., 2023a. Port integrated scheduling under uncertain operation time and cascade effects: A complex network structure entropy solution. Computers & Industrial Engineering 182, 109435. https://doi.org/10.1016/j.cie.2023.109435.

Cai, L., Li, W., Luo, Y., He, L., 2023b. Real-time scheduling simulation optimisation of job shop in a production-logistics collaborative environment. International Journal of Production Research 61, 1373–1393. https://doi.org/10.1080/00207543.2021.2023777.

Chang, D., Jiang, Z., Yan, W., He, J., 2010. Integrating berth allocation and quay crane assignments. Transportation Research Part e: Logistics and Transportation Review 46, 975–990. https://doi.org/10.1016/j.tre.2010.05.008.

Chen, X., He, S., Zhang, Y., Tong, L. (Carol), Shang, P., Zhou, X., 2020. Yard crane and AGV scheduling in automated container terminal: A multi-robot task allocation framework. Transportation Research Part C: Emerging Technologies 114, 241–271. https://doi.org/10.1016/j.trc.2020.02.012.

Chen, L., Langevin, A., Lu, Z., 2013. Integrated scheduling of crane handling and truck transportation in a maritime container terminal. European Journal of Operational Research 225, 142–152. https://doi.org/10.1016/j.ejor.2012.09.019.

Dik, G., Kozan, E., 2017. A flexible crane scheduling methodology for container terminals. Flex Serv Manuf J 29, 64–96. https://doi.org/10.1007/s10696-016-9264-4.

Expósito-Izquiero, C., Lalla-Ruiz, E., Lamata, T., Melián-Batista, B., Moreno-Vega, J.M., 2016. Fuzzy Optimization Models for Seaside Port Logistics: Berthing and Quay Crane Scheduling. In: Madani, K., Dourado, A., Rosa, A., Filipe, J., Kacprzyk, J. (Eds.), Studies in Computational Intelligence. Springer International Publishing, Cham, pp. 323–343. https://doi.org/10.1007/978-3-319-23392-5_18.

Fu, X., Pace, P., Aloi, G., Guerrieri, A., Li, W., Fortino, G., 2023. Tolerance Analysis of Cyber-Manufacturing Systems to Cascading Failures. ACM Trans. Internet Technol. https://doi.org/10.1145/3579847.

Guo, W., Atasoy, B., van Blokland, W.B., Negenborn, R.R., 2021. Global synchromodal transport with dynamic and stochastic shipment matching. Transportation Research Part e: Logistics and Transportation Review 152, 102404. https://doi.org/10.1016/j.tre.2021.102404.

Han, X., Lu, Z., Xi, L., 2010. A proactive approach for simultaneous berth and quay crane scheduling problem with stochastic arrival and handling time. European Journal of Operational Research 207, 1327–1340. https://doi.org/10.1016/j.ejor.2010.07.018.

He, J., 2016. Berth allocation and quay crane assignment in a container terminal for the trade-off between time-saving and energy-saving. Adv. Eng. Inform. 30, 390–405. https://doi.org/10.1016/j.aei.2016.04.006.

He, L., Li, W., Zhang, Y., Cao, Y., 2019b. A discrete multi-objective fireworks algorithm for flowshop scheduling with sequence-dependent setup times. Swarm and Evolutionary Computation 51, 100575. https://doi.org/10.1016/j.swevo.2019.100575.

He, L., Cao, Y., Li, W., Cao, J., Zhong, L., 2022. Optimization of energy-efficient open shop scheduling with an adaptive multi-objective differential evolution algorithm. Applied Soft Computing 118, 108459. https://doi.org/10.1016/j.asoc.2022.108459.

He, J., Huang, Y., Yan, W., Wang, S., 2015. Integrated internal truck, yard crane and quay crane scheduling in a container terminal considering energy consumption. Expert Systems with Applications 42, 2464–2487. https://doi.org/10.1016/j.eswa.2014.11.016.

He, J., Tan, C., Zhang, Y., 2019a. Yard crane scheduling problem in a container terminal considering risk caused by uncertainty. Advanced Engineering Informatics 39, 14–24. https://doi.org/10.1016/j.aei.2018.11.004.

He, J., Wang, Y., Tan, C., Yu, H., 2021. Modeling berth allocation and quay crane assignment considering QC driver cost and operating efficiency. Advanced Engineering Informatics 47, 101252. https://doi.org/10.1016/j.aei.2021.101252.

Hop, D.C., Van Hop, N., Anh, T.T.M., 2021. Adaptive particle swarm optimization for integrated quay crane and yard truck scheduling problem. Computers & Industrial Engineering 153, 107075. https://doi.org/10.1016/j.cie.2020.107075.

Hsu, H.-P., Tai, H.-H., Wang, C.-N., Chou, C.-C., 2021a. Scheduling of collaborative operations of yard cranes and yard trucks for export containers using hybrid approaches. Advanced Engineering Informatics 48, 101292. https://doi.org/10.1016/j.aei.2021.101292.

Hsu, H.-P., Wang, C.-N., Fu, H.-P., Dang, T.-T., 2021b. Joint Scheduling of Yard Crane, Yard Truck, and Quay Crane for Container Terminal Considering Vessel Stowage Plan: An Integrated Simulation-Based Optimization Approach. Mathematics 9, 2236. https://doi.org/10.3390/math9182236.

Ji, B., Tang, M., Wu, Z., Yu, S.S., Zhou, S., Fang, X., 2022. Hybrid rolling-horizon optimization for berth allocation and quay crane assignment with unscheduled vessels. Advanced Engineering Informatics 54, 101733. https://doi.org/10.1016/j.aei.2022.101733.

Jiang, E., Wang, L., Wang, J., 2021. Decomposition-based multi-objective optimization for energy-aware distributed hybrid flow shop scheduling with multiprocessor tasks. Tsinghua Science and Technology 26, 646–663. https://doi.org/10.26599/TST.2021.9010007.

Kaddani, S., Vanderpooten, D., Vanpeperstraete, J.-M., Aissi, H., 2017. Weighted sum model with partial preference information: Application to multi-objective optimization. European Journal of Operational Research 260, 665–679. https://doi.org/10.1016/j.ejor.2017.01.003.

Kaveh, A., Laknejadi, K., Alinejad, B., 2012. Performance-based multi-objective optimization of large steel structures. Acta Mech 223, 355–369. https://doi.org/10.1007/s00707-011-0564-1.

Kizilay, D., Hentenryck, P.V., Eliiyi, D.T., 2020. Constraint programming models for integrated container terminal operations. European Journal of Operational Research 286, 945–962. https://doi.org/10.1016/j.ejor.2020.04.025.

Lei, D., 2012. Co-evolutionary genetic algorithm for fuzzy flexible job shop scheduling. Applied Soft Computing 12, 2237–2245. https://doi.org/10.1016/j.asoc.2012.03.025.

Lei, M., Liu, L., Wei, D., 2019. An Improved Method for Measuring the Complexity in Complex Networks Based on Structure Entropy. IEEE Access 7, 159190–159198. https://doi.org/10.1109/ACCESS.2019.2950691.

Li, H., Lam, J.S.L., Yang, Z., Liu, J., Liu, R.W., Liang, M., Li, Y., 2022. Unsupervised hierarchical methodology of maritime traffic pattern extraction for knowledge discovery. Transportation Research Part c: Emerging Technologies 143, 103856. https://doi.org/10.1016/j.trc.2022.103856.
Li, H., Jiao, H., Yang, Z., 2023a. AIS data-driven ship trajectory prediction modelling and analysis based on machine learning and deep learning methods. Transportation Research Part e: Logistics and Transportation Review 175, 103152. https://doi.org/10.1016/j.tre.2023.103152.
Li, L., Li, Y., Liu, R., Zhou, Y., Pan, E., 2023b. A Two-stage Stochastic Programming for AGV scheduling with random tasks and battery swapping in automated container terminals. Transportation Research Part e: Logistics and Transportation Review 174, 103110. https://doi.org/10.1016/j.tre.2023.103110.
Li, H., Yang, Z., 2023. Incorporation of AIS data-based machine learning into unsupervised route planning for maritime autonomous surface ships. Transportation Research Part e: Logistics and Transportation Review 176, 103171. https://doi.org/10.1016/j.tre.2023.103171.
Liu, B., Li, Z.-C., Wang, Y., 2022. A two-stage stochastic programming model for seaport berth and channel planning with uncertainties in ship arrival and handling times. Transportation Research Part e: Logistics and Transportation Review 167, 102919. https://doi.org/10.1016/j.tre.2022.102919.
Liu, C., Zheng, L., Zhang, C., 2016. Behavior perception-based disruption models for berth allocation and quay crane assignment problems. Computers & Industrial Engineering 97, 258–275. https://doi.org/10.1016/j.cie.2016.04.008.
Lu, Y., Le, M., 2014. The integrated optimization of container terminal scheduling with uncertain factors. Computers & Industrial Engineering 75, 209–216. https://doi.org/10.1016/j.cie.2014.06.018.
Luan, D., Zhao, M., Zhao, Q., Wang, N., 2021. Modelling of integrated scheduling problem of capacitated equipment systems with a multi-lane road network. PLoS One 16, e0251875.
Ma, S., Li, H., Zhu, N., Fu, C., 2021. Stochastic programming approach for unidirectional quay crane scheduling problem with uncertainty. J Sched 24, 137–174. https://doi.org/10.1007/s10951-020-00661-8.
Ming, F., Gong, W., Wang, L., Gao, L., 2022. Constrained Multi-objective Optimization via Multitasking and Knowledge Transfer. IEEE Transactions on Evolutionary Computation 1–1. https://doi.org/10.1109/TEVC.2022.3230822.
Na, L., Zhihong, J., 2009. Optimization of Continuous Berth and Quay Crane Allocation Problem in Seaport Container Terminal, in: 2009 Second International Conference on Intelligent Computation Technology and Automation. Presented at the 2009 Second International Conference on Intelligent Computation Technology and Automation, pp. 229–233. https://doi.org/10.1109/ICICTA.2009.522.
Niu, Y., Yu, F., Yao, H., Yang, Y., 2022. Multi-equipment coordinated scheduling strategy of U-shaped automated container terminal considering energy consumption. Computers & Industrial Engineering 174, 108804. https://doi.org/10.1016/j.cie.2022.108804.
Rodrigues, F., Agra, A., 2021. An exact robust approach for the integrated berth allocation and quay crane scheduling problem under uncertain arrival times. European Journal of Operational Research 295, 499–516. https://doi.org/10.1016/j.ejor.2021.03.016.
Rouky, N., Abourraja, M., Boukachour, J., Boudebous, D., Alaoui, A., Khoukhi, F., 2019. Simulation optimization based ant colony algorithm for the uncertain quay crane scheduling problem. International Journal of Industrial Engineering Computations 10, 111–132.
Talley, W.K., Ng, M., 2022. Cargo port choice equilibrium: The case of shipping lines and cargo port service providers. Transportation Research Part e: Logistics and Transportation Review 164, 102817. https://doi.org/10.1016/j.tre.2022.102817.
Tan, C., He, J., 2021. Integrated proactive and reactive strategies for sustainable berth allocation and quay crane assignment under uncertainty. Ann Oper Res. https://doi.org/10.1007/s10479-020-03891-3.
Tan, C., Yan, W., Yue, J., 2021. Quay crane scheduling in automated container terminal for the trade-off between operation efficiency and energy consumption. Advanced Engineering Informatics 48, 101285. https://doi.org/10.1016/j.aei.2021.101285.
Xiang, X., Liu, C., Miao, L., 2017. A bi-objective robust model for berth allocation scheduling under uncertainty. Transportation Research Part e: Logistics and Transportation Review 106, 294–319. https://doi.org/10.1016/j.tre.2017.07.006.
Xiang, X., Liu, C., Miao, L., 2018. Reactive strategy for discrete berth allocation and quay crane assignment problems under uncertainty. Computers & Industrial Engineering 126, 196–216. https://doi.org/10.1016/j.cie.2018.09.033.
Xin, J., Negenborn, R.R., Lodewijks, G., 2014. Energy-aware control for automated container terminals using integrated flow shop scheduling and optimal control. Transportation Research Part c: Emerging Technologies 44, 214–230. https://doi.org/10.1016/j.trc.2014.03.014.
Xin, J., Negenborn, R.R., Corman, F., Lodewijks, G., 2015. Control of interacting machines in automated container terminals using a sequential planning approach for collision avoidance. Transportation Research Part c: Emerging Technologies 60, 377–396. https://doi.org/10.1016/j.trc.2015.09.002.
Xu, B., Jie, D., Li, J., Yang, Y., Wen, F., Song, H., 2021. Integrated scheduling optimization of U-shaped automated container terminal under loading and unloading mode. Computers & Industrial Engineering 162, 107695. https://doi.org/10.1016/j.cie.2021.107695.
Xu, B., Jie, D., Li, J., Zhou, Y., Wang, H., Fan, H., 2022. A Hybrid Dynamic Method for Conflict-Free Integrated Schedule Optimization in U-Shaped Automated Container Terminals. Journal of Marine Science and Engineering 10, 1187. https://doi.org/10.3390/jmse10091187.
Yang, M., Li, C., Tang, Y., Wu, W., Zhang, X., 2024. A collaborative resequencing approach enabled by multi-core PREA for a multi-stage automotive flow shop. Expert Systems with Applications 237, 121825. https://doi.org/10.1016/j.eswa.2023.121825.
Yang, Y., Zhong, M., Dessouky, Y., Postolache, O., 2018. An integrated scheduling method for AGV routing in automated container terminals. Computers & Industrial Engineering 126, 482–493. https://doi.org/10.1016/j.cie.2018.10.007.
Yu, J., Voß, S., Cammin, P., 2021. Integrating vessel arrival time prediction having interval uncertainty into the berth allocation and quay crane assignment. Presented at the Transportation Research Board 100th Annual Meeting Transportation Research Board.
Yu, J., Tang, G., Voß, S., Song, X., 2023. Berth allocation and quay crane assignment considering the adoption of different green technologies. Transportation Research Part e: Logistics and Transportation Review 176, 103185. https://doi.org/10.1016/j.tre.2023.103185.
Yuan, X., Zhang, B., Wang, P., Liang, J., Yuan, Y., Huang, Y., Lei, X., 2017. Multi-objective optimal power flow based on improved strength Pareto evolutionary algorithm. Energy 122, 70–82. https://doi.org/10.1016/j.energy.2017.01.071.
Yue, L.-J., Fan, H.-M., Fan, H., 2023. Blocks allocation and handling equipment scheduling in automatic container terminals. Transportation Research Part c: Emerging Technologies 153, 104228. https://doi.org/10.1016/j.trc.2023.104228.
Zeng, Q., Yang, Z., 2009. Integrating simulation and optimization to schedule loading operations in container terminals. Computers & Operations Research 36, 1935–1944. https://doi.org/10.1016/j.cor.2008.06.010.
Zhang, Y., Guo, W., Negenborn, R.R., Atasoy, B., 2022b. Synchromodal transport planning with flexible services: Mathematical model and heuristic algorithm. Transportation Research Part c: Emerging Technologies 140, 103711. https://doi.org/10.1016/j.trc.2022.103711.
Zhang, H.L., Jiang, Z.B., 2008. Simulation Studies of Heuristic Approaches for Dynamic Scheduling of Container Terminal Operations. International Journal of Modelling and Simulation 28, 410–422. https://doi.org/10.1080/02286203.2008.11442494.
Zhang, R., Jin, Z., Ma, Y., Luan, W., 2015. Optimization for two-stage double-cycle operations in container terminals. Computers & Industrial Engineering 83, 316–326. https://doi.org/10.1016/j.cie.2015.02.007.
Zhang, X., Li, H., Wu, M., 2022a. Optimization of Resource Allocation in Automated Container Terminals. Sustainability 14, 16869. https://doi.org/10.3390/su142416869.
Zhang, S., Lv, M., Dai, J., Li, Y., 2020b. Research on quay crane scheduling optimization based on the uncertainty of operation time. Industrial Engineering and Management 25, 50–58.
Zhang, B., Pan, Q.-K., Gao, L., Meng, L.-L., Li, X.-Y., Peng, K.-K., 2020a. A Three-Stage Multiobjective Approach Based on Decomposition for an Energy-Efficient Hybrid Flow Shop Scheduling Problem. IEEE Transactions on Systems, Man, and Cybernetics: Systems 50, 4984–4999. https://doi.org/10.1109/TSMC.2019.2916088.
Zhen, L., Hu, H., Wang, W., Shi, X., Ma, C., 2018. Cranes scheduling in frame bridges based automated container terminals. Transportation Research Part c: Emerging Technologies 97, 369–384. https://doi.org/10.1016/j.trc.2018.10.019.
Zhen, L., Yu, S., Wang, S., Sun, Z., 2019. Scheduling quay cranes and yard trucks for unloading operations in container ports. Ann Oper Res 273, 455–478. https://doi.org/10.1007/s10479-016-2335-9.

Zhen, L., Zhuge, D., Wang, S., Wang, K., 2022. Integrated berth and yard space allocation under uncertainty. Transportation Research Part b: Methodological 162, 1–27. https://doi.org/10.1016/j.trb.2022.05.011.

Zheng, F., Man, X., Chu, F., Liu, M., Chu, C., 2019. A two-stage stochastic programming for single yard crane scheduling with uncertain release times of retrieval tasks. International Journal of Production Research 57, 4132–4147. https://doi.org/10.1080/00207543.2018.1516903.

Zhong, M., Yang, Y., Zhou, Y., Postolache, O., 2019. Adaptive Autotuning Mathematical Approaches for Integrated Optimization of Automated Container Terminal. Mathematical Problems in Engineering 2019, 1–14. https://doi.org/10.1155/2019/7641670.

Zhou, C., Lee, B.K., Li, H., 2020. Integrated optimization on yard crane scheduling and vehicle positioning at container yards. Transportation Research Part e: Logistics and Transportation Review 138, 101966. https://doi.org/10.1016/j.tre.2020.101966.

Zhu, G.-Y., He, L.-J., Ju, X.-W., Zhang, W.-B., 2018. A fitness assignment strategy based on the grey and entropy parallel analysis and its application to MOEA. European Journal of Operational Research 265, 813–828. https://doi.org/10.1016/j.ejor.2017.08.022.

Zhu, S., Tan, Z., Yang, Z., Cai, L., 2022. Quay crane and yard truck dual-cycle scheduling with mixed storage strategy. Advanced Engineering Informatics 54, 101722. https://doi.org/10.1016/j.aei.2022.101722.

Zhuang, Z., Zhang, Z., Teng, H., Qin, W., Fang, H., 2022. Optimization for integrated scheduling of intelligent handling equipment with bidirectional flows and limited buffers at automated container terminals. Computers & Operations Research 145, 105863. https://doi.org/10.1016/j.cor.2022.105863.